MONTHLY NOTICES

OF THE

ROYAL ASTRONOMICAL SOCIETY

Vol. 101 No. 7

MEETING OF 1941 JULY 11

Professor S. Chapman, President, in the Chair

The election by the Council of the following Fellow was duly confirmed:—

Colonel Frederick William Nicholls, Staddle Barn Cottage, Coombe Bisset, Wilts.

Thirty-six presents were announced as having been received since the last meeting.

The Secretary read a letter from the Physical Society, inviting Fellows of the Royal Astronomical Society to be present at a meeting on July 25 at the Science Museum, when the first Charles Chree Medal and Prize would be presented to Professor Sydney Chapman, President, R.A.S., in recognition of his work on Geomagnetism and the Upper Atmosphere.

MEETING OF 1941 SEPTEMBER 12

Professor S. Chapman, President, in the Chair

The election by the Council of the following Fellow was duly confirmed:—

Alan William James Cousins, 27 Exmouth Avenue, Upper Glenwood, Durban, S. Africa.

The following candidates were proposed for election as Fellows of the Society, the names of the proposers from personal knowledge being appended:—

Derrick Stanley Box, Woollhara, 63 Warwick Road, Thornton Heath, Surrey (proposed by A. D. Thackeray); and

Henry Welsh, Littlecote, Widemouth Bay, near Bude, Cornwall (proposed by F. J. Sellers).

Forty-two presents were announced as having been received since the last ordinary meeting, including

Utrecht Observatory, Photometric Atlas of the Solar Spectrum from λ 3612 to λ 8771, with an Appendix from λ 3332 to λ 3637. By M. Minnaert, G. F. W. Mulders and J. Houtgast.

THE INTENSITIES OF A TRIPLET OF *Si*III IN EARLY-TYPE SPECTRA

I. H. Abdel-Rahman, Ph.D.

(Communicated by Professor W. M. H. Greaves)

(Received 1941 July 21)

The three *Si*III lines, $\lambda\lambda$ 4552, 4567 and 4574 form a triplet; their theoretical intensities, according to the summation rules, are 5 : 3 : 1 respectively. They reach maximum intensity between B1–B2, and are usually absent outside the spectral range B3–O9. The equivalent widths of the lines were first measured by Struve and Elvey *, who found that the relative intensities agree with the square roots of the above ratios, and that there is no difference in this respect between stars with wide and sharp lines. From this they concluded that the lines are formed mainly by radiation damping and that axial rotation is responsible for the broadening of the lines and not any peculiar form of absorption coefficient. The total intensities were subsequently re-examined by Elvey † for differences in "gradient" between high and low luminosity stars. He found deviations from the square root ratios without, however, attributing them to luminosity effect. E. G. Williams ‡ and P. Rudnick § published lists of the total intensities of the lines in many B-type stars, but neither of them discussed the relative intensities. Their measures will be referred to in this note.

The agreement with the square root ratios indicates that the lines should fall on the natural damping section of the appropriate curve of growth. Few absorption lines are observed in B-type stars, and still fewer of these are of known theoretical strength or can be grouped in multiplets. Goldberg || has used Williams's ¶ measures together with a mean theoretical curve of growth for B-type stars to study the absorption lines of *He*I, *N*II and *O*II. All these were found to fall either on the Doppler or the intermediate part of the curve, and since the *Si*III lines are expected to be on the damping part, it becomes of interest to see whether the *Si*III lines can be represented by the same curve used by Goldberg. The procedure of assuming a mean theoretical curve and comparing it with the few available observations is admittedly uncertain, but with the present accuracy of measurement the order of magnitude of the results should be reliable. The purpose of the present note is to examine the relative intensities of the *Si*III lines in relation to luminosity, line width and spectral type, and to discuss the formation of the lines.

The material consists of 79 spectra of 31 stars, photographed on 50 plates. They form a part of the programme of measuring the total line intensities in early-type stars, which is in progress at the Royal Observatory, Edinburgh. All the plates were secured with the two-prism spectrograph attached to the 36-inch reflector, giving a linear dispersion 36 A./mm. at 4567 A. Ilford Astra VIII plates were used. Calibration was made with a multiplet-slit spectrograph, neutral filters being introduced so as to obtain densities comparable with those in the star's spectrum. For plates taken on or subsequent to 1939 February 6 equal exposure times were used in photographing the stellar and calibration spectra. For previous plates a correcting factor was introduced to allow for time effect.** The measurements were made on a direct-reading micro-photometer of the Moll type, the calibrations being measured at ten points near to the *Si*III triplet corresponding in mean wave-length to 4567 A.

The new measures are given in Table I. The luminosity characteristics *g* (giant),

* *Ap. J.*, 72, 267, 1930. † *Ap. J.*, 78, 219, 1933. ‡ *Ap. J.*, 83, 279, 1936.
§ *Ap. J.*, 83, 439, 1936. || *Ap. J.*, 89, 623, 1939. ¶ *Loc. cit.* ** *M.N.*, 96, 825, 1936.

i (intermediate) and *d* (dwarf) are taken from the lists of Struve, Williams, Rudnick and others. The total absorption in the fourth column is the sum of the intensities of the three lines in units of ·01 A. of the continuous spectrum. The last three columns give the relative intensities of the lines (referred to a total of 100).

TABLE I

Star	No. of Plates	Type	Total Intensity (·01 A.)	Relative Intensities 4552	4567	4574	Star	No. of Plates	Type	Total Intensity (·01 A.)	Relative Intensities 4552	4567	4574
γ Peg	5	B2*d*	58	45	31	24	ζ Ori	1	Bo*d*	30	47	33	20
κ Cas	6	Bo*ei*	130	41	38	21	ρ Leo	1	Bo*g*	134	45	31	24
ζ Cas	3	B2*d*	47	46	29	25	102 Her	1	B3*d*	32	62	13	25
ξ Cas	1	B3	19	42	37	21	η Lyr	1	B3*i*	39	38	41	21
o Cas	1	B2*e*	33	36	36	28	b^2 Cyg	1	B2*e*	20	40	40	20
δ Cet	4	B2	63	48	31	21	P Cyg	3	B1	135	47	32	21
35 Ari	1	B3	21	48	31	21	55 Cyg	8	B2*g*	99	44	32	24
40 Per	1	B2*i*	37	49	34	17	ν Cyg	3	B3*e*	35	49	30	21
o Per	3	B1	123	46	30	24	β Cep	4	B1*d*	92	41	35	24
ζ Per	8	B1*g*	122	43	35	22	9 Cep	3	B2*g*	87	46	32	22
ϵ Per	6	B3*d*	82	44	35	21	π^2 Cyg	1	B3*i*	58	41	45	14
λ Tau	1	B3*d*	31	45	32	23	6 Lac	1	B3*i*	92	51	35	14
9 Cam	1	Bo*eg*	24	50	21	29	10 Lac	1	Oe5*d*	35	55	20	35
η Aur	3	B3*d*	35	36	35	29	1 Cas	2	B1*i*	106	39	34	27
γ Ori	1	B2*d*	76	55	26	19	σ Cas	2	B2	62	39	39	22
λ Ori	1	Oe5*g*	26	46	27	27							

Table II summarises the results of different observers. Every series is given weight equal to the number of spectra measured. The final mean ratios agree very closely with the square root ratios. The deviation for λ 4552 is negligible, while for the other two lines it may be partly real. Blending with other faint absorption lines, neglect of Doppler core correction and errors of measurement possibly contribute to these deviations.

As regards the Edinburgh measures, all the plates were developed and brushed under similar conditions. Measurements on the photometer were extended from λ 4500 to λ 4625 to ensure a reliable determination of continuous spectrum.

TABLE II

*Mean Relative Intensities of Si*III *Lines*

Observer	No.	λ 4552	λ 4567	λ 4574
Emission spark (Struve and Elvey)	4	53·1	32·4	13·5
Stellar observations by Struve and Elvey	12	46·7	31·1	22·2
,, ,, ,, Elvey	26	41·0	34·4	24·6
,, ,, ,, Williams	26	46·2	35·0	18·8
,, ,, ,, Rudnick	31	45·9	32·4	21·7
Mean of above stellar ratios	95	44·6	33·4	21·8
Edinburgh observations	79	44·4	33·0	22·6
Final mean	174	44·6	33·2	22·2
Theoretical multiplet ratios	...	55·6	33·3	11·1
Square roots of multiplet ratios	...	45·0	34·9	20·1
Deviation of final mean from $\sqrt{-}$ ratios	...	− ·4	− 1·7	+ 2·1
,, ,, ,, direct ratios	...	−11·0	− ·1	+11·1

From an investigation of the measures of κ Cas (6 plates), ζ Per (8 plates), ϵ Per (6 plates) and 55 Cyg (8 plates), it appears that there is no correlation between measured total absorption and density of spectrum, and this circumstance is reassuring as far as possible systematic error from photographic causes is concerned. The average probable error of a single measurement of intensity is found to be $\pm$ 10 per cent. This includes the contribution made by erroneous fixing of the continuous spectrum, and systematic errors due to scattered light, both of which do not affect the relative intensities appreciably, and therefore the probable errors of the relative intensities are considered to be less than 10 per cent.

The only effective possibility of blending seems to be a blend of λ 4552 with two faint lines of *N*II and *S*II whose identification is, however, uncertain. By comparing their (laboratory) intensities with those of other lines of the same elements in the same stars it is estimated that the increase in intensity of λ 4552 due to blending in stars with strong *Si*III lines is not more than one unit on the visual scale used by Struve * and Marshall †, corresponding to about ·05 A. total absorption. It should be noticed that any such small increase of λ 4552 would make the deviations of the observed relative intensities from the square root ratios proportional to $+55 : -35 : -20$—that is, the relative intensities of λ 4567 and λ 4574 would be decreased respectively by ·64 and ·36 times the increase of the relative intensity of λ 4552.‡ The observed deviations (Table II) do not agree with this and cannot thus be ascribed solely to the effect of blending on λ 4552. Doppler correction would affect fainter lines to a greater extent and would produce for stars in which *Si*III is weak relative intensities which would be greater for λ 4552 and less for λ 4574 than the square root ratios. The values of s/f (see below) in Table III are not in accord with this.

The stars were then grouped according to line width, luminosity, spectral type and strength of the lines. The relative intensities in each group in all of the five series of observations discussed were found to agree with the theoretical ratios within the expected errors considering the small number of observations and the statistical nature of the discussion.

The results are given in Table III in the form of the ratios between the mean relative intensities of each line in strong-line stars (s) to that in the faint-line stars (f). Each series of observations is treated separately and therefore the final ratios in the table are comparable. Similar values are given for the giant (g) and the dwarf (d) groups. The mean in the last column is weighted according to the number of spectra.

TABLE III

Line	Ratio	Struve and Elvey	Elvey	Williams	Rudnick	Edinburgh	Mean
λ 4552	s/f	·989	1·010	·910	·923	·960	·955
	g/d	·989	1·017	·966	·951	·982	·980
λ 4567	s/f	1·048	1·066	1·154	1·111	1·075	1·090
	g/d	1·048	1·047	1·043	1·081	1·027	1·044
λ 4574	s/f	·957	·899	·967	1·023	·973	·969
	g/d	·957	·910	1·016	·981	1·004	·984

There appears to be a one to one correspondence between the s/f and g/d values. This indicates that the high luminosity stars have usually strong *Si*III lines. Incidentally

* *Ap. J.*, 74, 225, 1931. † *Publ. Michigan*, V, 137, 1934.

‡ If the true equivalent breadths of the lines are 45I, 35I and 20I, then the effect of blending on λ 4552 would be to make the measured equivalent breadth $45\text{I} + x$. The deduced relative intensities would then be $f(45\text{I} + x)$, $35f\text{I}$ and $20f\text{I}$, where the factor f is chosen so as to make the sum of the relative intensities equal to 100. For small x these become $45 + 55x/100\text{I}$, $35 - 35x/100\text{I}$ and $20 - 20x/100\text{I}$, so that the deviations from the relative intensities 45, 35 and 20 corresponding to the square roots of multiplet ratios are proportional to $+55 : -35 : -20$.

this confirms the general basis on which the luminosity groups of B-type stars are based. Table III does not reveal any systematic tendency towards steeper gradients for giants. The mean relative intensities of λλ 4552, 4567 and 4574 are 43·4, 34·9, 21·7 and 45·0, 32·3, 22·7 for strong-lined and weak-lined stars respectively, whilst for the high and low luminosity groups the values are 43·8, 34·3, 22·0 and 44·9, 32·8, 22·3. λλ 4574 and 4552 are relatively stronger in faint-lined and in dwarf stars, while λ 4567 is relatively weaker. This effect is more conspicuous in the *s*/*f* ratios than in the *g*/*d*, suggesting that the true explanation is connected with the total absorption of the lines rather than with the luminosity of the star. There is no correlation between relative intensities and spectral type or line width, confirming Struve and Elvey's conclusion.

The observational conclusion is that the total intensities of the lines in the *Si*III triplet are approximately proportional to the square roots of the theoretical intensities in emission derived from the summation rules. The small deviations which have been found from the square root ratios may possibly be attributed to the effect of instrumental scattering, complicated perhaps by small deviations due to Doppler correction and blending. But the deviations are small, and there seems to be no reason to doubt the main conclusion that the observed intensities are in good agreement with the square root ratios.

The inference would appear to be that on the appropriate curve of growth the *Si*III lines fall on the damping section, the equivalent widths being large enough to place the lines beyond the intermediate part of the curve. To estimate the minimum equivalent width of the lines so as to satisfy this condition, the theoretical curve of growth given by Goldberg * was used. Allowing for the difference in atomic weight between helium and silicon, we find that damping operates for lines of total absorption $> \cdot 30$ A. This value was checked by two other curves by Minnaert and Slob † and by v. d. Held (reproduced by Unsöld) ‡ which gave the limiting values of ·28 A. and ·30 A. respectively. But these values, which are based on theoretical curves incorporating assumed values for the damping constant and for the Doppler width, seem to be in disagreement with the measured total intensities. Table IV gives the mean total absorption for stars with strong and faint lines. It will be noticed that all the lines in the weak-line group are below the limit, but the (weighted) mean intensities for this group are 18·2, 13·1 and 9·2, the corresponding relative intensities being 45·0, 32·3 and 22·7 in good agreement with the square roots of the theoretical emission intensities. All the lines (except λλ 4552 and 4567 in the strong-line group) are below the limit.

TABLE IV

Mean Total Absorptions of SiIII Lines

(Unit ·01 A.)

Observer	Stars with Strong Lines				Stars with Faint Lines			
	No. of Spectra	4552	4567	4574	No. of Spectra	4552	4567	4574
Struve and Elvey	6	46	34	23	6	20	13	10
Elvey	13	40	35	23	13	15	12	10
Williams	13	54	46	23	13	21	16	9
Rudnick	16	40	31	20	15	13	9	6
Edinburgh	37	47	37	24	42	20	14	10

* *Loc. cit.* † *Procs. Acad. Amsterdam*, 34, 442, 1931.

‡ Unsöld, *Physik der Sternatmosphären*, p. 168.

To secure agreement with the theory as it stands it would have to be assumed that the measured total intensities of the fainter lines are only a fraction (one-third in some cases) of the true values. Such an assumption is inadmissible and thus it appears that the flat portion of the theoretical curve has to be lowered, involving either an excessively small Doppler width or an excessively large damping constant. If the latter explanation is the correct one, it is found from Minnaert and Slob's curve that the damping constant should be of the order of 450 times the classical value. This figure could be lowered somewhat by assuming that the measured equivalent widths are systematically small, but it does seem that the observational results give rise to difficult theoretical considerations.

In conclusion it is a pleasure to record thanks to Professor W. M. H. Greaves for his kind help and advice and also to the staff of the Observatory.

Summary

The total intensities of the three lines in a *Si*III triplet have been measured in 31 early-type stars. The results confirm the conclusion previously found that the intensities are approximately proportional to the square roots of the theoretical emission intensities. It is noticed that when the result is discussed in the light of existing theory there is a discrepancy which may possibly be explained by assuming a large damping constant. The relative intensities of the lines are discussed with regard to luminosity and total absorption.

A CRITICAL EXAMINATION OF THE LEANDER McCORMICK PROPER MOTIONS

A. Ali, M.A., B.Sc.

(Communicated by the Director, University Observatory, Glasgow)

(Received 1941 July 7)

1. The present paper is the result of the preliminary work done in connection with the study of proper motions of the faint stars in the Publication of the Leander McCormick Observatory, vol. vii (1937), on the basis of the two-streams theory; the alternative ellipsoidal hypothesis has been already investigated by van de Kamp and Vyssotsky.

In each photographic region, the authors have reduced the relative motions to absolute motions in two ways*, by applying the correction (1) the absolute motion minus the relative motion of one or more Boss stars, (2) parallactic motion minus mean relative motion of all the stars in the region. These two corrections are given in the publication at the head of each region with their weights. The two reductions are, however, for several regions so discordant that it is questionable whether even their weighted mean can serve any useful purpose. Further, in the second method, the galactic rotational effects have not been allowed for and the method itself as employed by the authors is not entirely independent of the first method. Therefore, in the second method, I have used, instead of the parallactic motion, the systematic motions given by van Rhijn and Bok.† These motions are in seconds of arc per annum,

$$\left.\begin{aligned} \pi_x &= P\left(\frac{\bar{h}}{\rho}\right)_m + Q \text{ in R.A.,} \\ \pi_y &= P'\left(\frac{\bar{h}}{\rho}\right)_m + Q' \text{ in Dec.,} \end{aligned}\right\} \qquad (1)$$

where Q and Q' are the rotational effects, $\left(\frac{\bar{h}}{\rho}\right)_m$ is the secular parallax which is a function of Harvard visual magnitude and galactic latitude, and P and P' depend on the equatorial co-ordinates of the star and the solar apex ($18^h{\cdot}0 + 31°{\cdot}0$). The values of P, P', Q, Q' and $\left(\frac{\bar{h}}{\rho}\right)_m$ are given by van Rhijn and Bok. The McCormick magnitudes (*IPv*) were reduced to the Harvard visual scale by means of formulæ given by Seares.‡

2. Three groups, Nos. 21, 32 and 40 (Appendix V, Table V, 1, p. 63, of the McCormick Publication), with a total of about 2100 stars were chosen sufficiently far apart from each other to give a fair idea of the preferential motions. The positional co-ordinates and other relevant data regarding the regions in each group are given in Table I.

In each region the absolute proper motions were counted in the sector $\theta - 5°$, $\theta + 5°$, where θ is the position angle of a proper motion and smoothed in the usual way. The form of the frequency curve was found to be very sensitive with regard to the position of the absolute origin in each region; therefore, three "absolute" origins were employed in each region and their respective frequency curves were obtained as indicated above. The three "absolute" origins were determined as follows:—

(*a*) The absolute origin (ξ_a, η_a) with respect to the origin of the relative motions

* *Publication of Leander McCormick Observatory*, 7, p. 14, 1937.

† *Groningen Publication*, No. 45, 1931.

‡ *Mt. Wilson Contr.*, No. 287, p. 1; No. 288, pp. 4 and 5; No. 289, p. 7.

TABLE I

Co-ordinates of the Groups and Regions

Group	Group Centre R.A.	Group Centre Dec.	Region	Regional Centre R.A.	Regional Centre Dec.	Gal. Lat.	No. of Stars in Region	Total No. of Stars
	°	°		h m	° ′	°		
21	312	+56	267	20 03·6	+52 52	+10	55	667
			273	20 10·5	+46 26	+ 6	111	
			276	20 15·9	+55 05	+10	252	
			285	20 43·3	+61 27	+11	83	
			295	21 16·2	+62 10	+ 8	65	
			311	22 07·4	+57 42	0	101	
32	289	− 2	237	18 56·3	− 5 53	− 3	305	648
			241	19 00·9	− 5 02	− 3	75	
			248	19 20·5	+ 2 55	− 4	162	
			260	19 47·4	+ 0 45	+11	106	
40	9	+55	340	23 49·4	+56 57	− 6	143	838
			1	0 03·8	+58 36	− 6	70	
			8	0 34·8	+55 59	− 9	179	
			11	0 43·0	+57 17	− 8	145	
			15	1 05·0	+54 37	−10	143	
			17	1 21·7	+44 53	−19	158	

TABLE II

Co-ordinates of the Absolute Origin (ξ, η)

(Unit = 0″·001)

Group	Region	ξ_a	η_a	ξ_b	η_b	ξ_c	η_c
21	267	−10	+ 7	−3	+ 2	−7	+ 5
	273	− 3	−10	0	0	−2	− 5
	276	− 4	− 4	+2	+ 5	−1	+ 1
	285	0	− 4	+1	+ 1	+1	− 2
	295	− 4	0	−1	+ 3	−3	+ 2
	311	−10	− 3	−4	+ 3	−7	0
32	237	+ 6	− 4	+5	− 2	+6	− 3
	241	+ 7	+12	+3	+16	+5	+14
	248	− 5	− 1	0	+ 7	−2	+ 3
	260	− 1	+ 2	−1	+ 5	−1	+ 3
40	340	− 7	+ 1	−2	+ 3	−5	+ 2
	1	−11	− 1	−5	+ 1	−8	0
	8	− 9	− 3	−2	0	−6	− 2
	11	− 9	− 1	−6	+ 5	−8	+ 2
	15	− 6	+ 2	−3	+ 2	−5	+ 2
	17	− 1	+ 5	−3	+ 7	−2	+ 6

in each region is the weighted mean of the two reductions to absolute motions, with signs reversed, in R.A. and declination given in the Publication at the head of each region.

(*b*) The absolute origin (ξ_b, η_b) is derived by means of the equations

$$\left.\begin{aligned} N\xi_b &= \Sigma\mu_x - N\pi_x, \\ N\eta_b &= \Sigma\mu_y - N\pi_y, \end{aligned}\right\} \qquad (2)$$

where π_x, π_y are the annual systematic motions obtained from (1); μ_x, μ_y are the relative proper motions in R.A. and declination, and N is the number of the stars in each magnitude group. Large relative motions were rejected in each magnitude group whenever

$$|\,\mu_{x \text{ or } y}\,| > 3 \times |\,\overline{\mu_{x \text{ or } y}}\,|$$

and the magnitude groups were restricted to $m \leqslant 12^{m}.0$ (except for group 40, where $m \leqslant 12^{m}.5$) in order to eliminate the influence of errors of measurement of the fainter stars. The values of ξ_b, η_b thus obtained are the weighted mean of several magnitude groups.

(*c*) The co-ordinates of the absolute origin (ξ_c, η_c) are the simple mean between (ξ_a, η_a) and (ξ_b, η_b).

The co-ordinates of the three "absolute" origins as outlined above are given in Table II.

3. The frequency curves for group 21 with the "absolute" origin at (ξ_a, η_a), (ξ_b, η_b), (ξ_c, η_c) are shown in fig. 1. The distribution of the proper motions in position angle

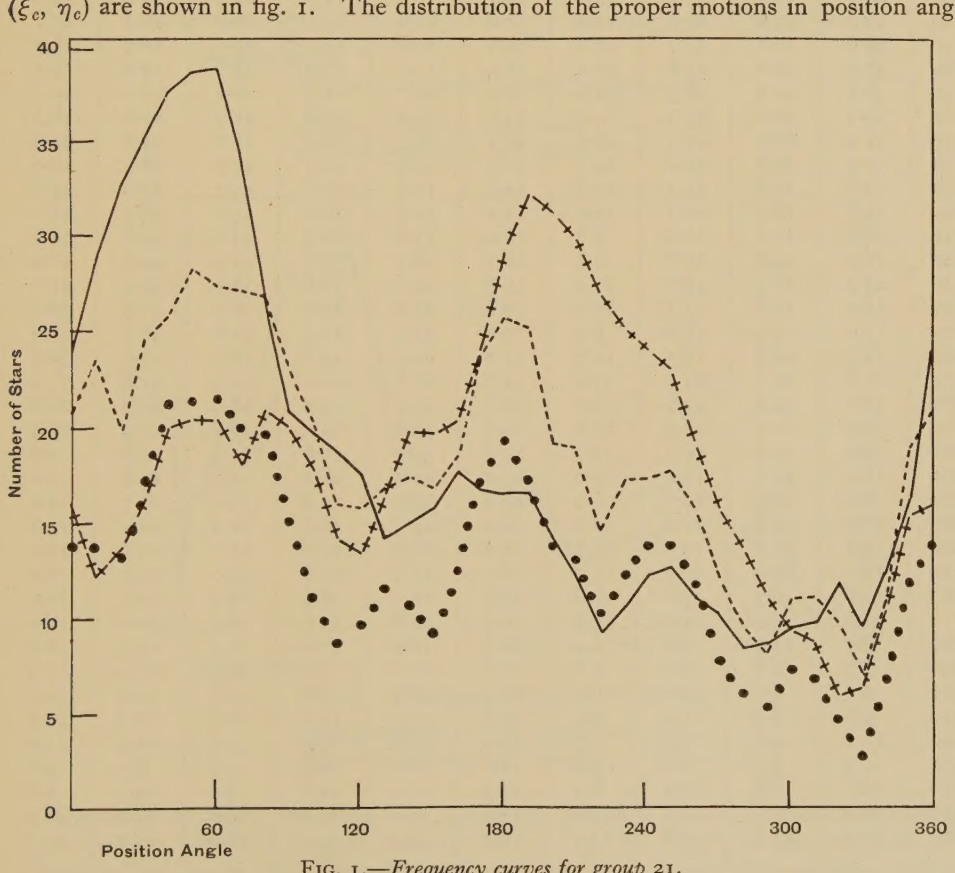

FIG. 1.—*Frequency curves for group 21.*

Absolute origin (ξ_a, η_a); *curve* ————
Absolute origin (ξ_b, η_b); *curve* + + + + +
Absolute origin (ξ_c, η_c); *curve* – – – – –

is given for the three groups in Table III, where ρ_a, ρ_b, ρ_c are the smoothed numbers of "absolute" proper motions in a 10° sector counted with respect to the absolute origin at (ξ_a, η_a), (ξ_b, η_b) and (ξ_c, η_c). The strong variation in the three curves as shown in fig. 1 suggested that errors in small proper motions might be responsible for it. Therefore, for group 21, all centennial proper motions less than 1″ were neglected when counting the proper motions in each 10° sector with "absolute" origin at (ξ_c, η_c). This reduced distribution is given in Table III under ρ_c', and its corresponding frequency curve is shown in fig. 1 by dots. The similarity between the two curves under ρ_c and ρ_c' proves that the small proper motions are not to be blamed.

TABLE III

Distribution of Proper Motions in Position Angle

θ	Group 21				Group 32			Group 40		
	ρ_a	ρ_b	ρ_c	ρ_c'	ρ_a	ρ_b	ρ_c	ρ_a	ρ_b	ρ_c
°										
10	28·8	12·2	23·5	13·8	15·7	10·7	13·0	14·5	9·7	13·8
20	33·2	13·8	19·8	13·3	16·0	11·0	13·0	18·0	10·3	15·7
30	35·0	16·2	24·7	17·2	15·7	10·8	12·5	20·0	12·3	16·5
40	37·5	20·0	25·8	21·2	16·3	11·0	13·3	24·3	15·2	19·5
50	38·5	20·2	28·3	21·2	16·5	10·7	13·3	26·2	17·0	21·7
60	38·7	20·2	27·5	21·5	21·2	14·2	16·8	31·3	20·0	28·3
70	34·7	18·0	27·3	20·0	22·3	17·3	18·3	36·7	23·0	32·3
80	27·0	20·8	27·0	19·7	21·2	19·3	19·3	49·7	28·5	40·0
90	20·8	20·0	23·3	15·0	15·3	17·7	16·7	53·7	33·0	42·8
100	19·7	18·3	20·3	11·0	17·5	15·0	16·0	55·0	38·5	47·0
110	18·8	14·2	16·0	8·7	16·0	13·8	16·3	44·8	40·0	44·7
120	17·5	14·0	15·8	9·7	16·7	16·5	16·3	43·5	44·5	44·2
130	14·3	16·3	16·8	11·5	16·8	20·7	17·8	38·5	39·5	41·7
140	15·0	19·8	17·3	10·7	17·8	25·0	19·0	36·0	41·3	38·0
150	15·7	19·7	16·8	9·3	19·8	24·5	21·3	31·8	38·5	35·2
160	17·7	20·3	18·5	12·5	15·0	23·3	20·7	28·7	37·2	30·5
170	16·8	23·7	23·7	17·0	15·5	20·8	20·0	24·3	34·2	31·2
180	16·5	29·3	25·7	19·3	18·0	30·0	23·2	18·0	29·8	26·3
190	16·5	32·2	25·3	17·7	25·0	35·2	29·2	16·7	29·3	24·5
200	14·2	31·3	19·3	13·7	27·8	39·0	31·8	15·3	25·2	19·0
210	12·2	30·0	19·0	13·0	25·7	28·2	28·2	13·3	22·5	17·0
220	9·2	27·0	14·7	10·3	20·7	23·5	21·5	13·2	21·7	15·2
230	10·5	25·3	17·2	12·2	17·7	19·5	19·2	12·3	22·5	15·8
240	12·2	24·3	17·3	13·7	18·0	22·7	22·3	13·7	23·0	16·0
250	12·7	23·0	17·7	13·7	20·0	18·7	21·8	15·7	23·0	18·8
260	11·0	19·3	15·8	11·8	18·5	16·2	18·3	18·3	22·7	18·0
270	10·2	15·7	12·0	7·7	16·5	14·8	15·0	18·5	22·0	19·0
280	8·5	13·7	9·7	6·0	16·7	16·3	17·0	15·3	19·7	16·0
290	8·7	11·3	8·0	5·3	17·7	16·0	17·0	12·7	16·3	13·3
300	9·5	9·3	11·0	7·2	20·5	15·3	18·0	11·8	15·0	12·0
310	9·8	8·7	11·0	5·7	17·0	13·3	14·7	10·7	12·3	10·8
320	11·7	5·7	9·7	4·7	15·7	14·0	15·5	11·0	11·3	11·7
330	9·5	6·3	7·0	2·8	11·7	10·3	12·7	9·7	8·0	9·7
340	12·3	10·8	10·3	6·7	12·3	10·3	12·7	9·2	10·3	8·8
350	16·3	15·2	18·8	11·8	15·0	10·0	13·2	9·7	10·0	10·0
360	24·0	15·7	20·8	13·7	16·7	10·3	13·0	13·0	10·7	12·0

The same strong variation is also found usually in the individual regions of each group. Figs. 2A, 2B show the curves for the two regions 276, 295 of the group 21.

The curves are drawn with the absolute origins at (ξ_a, η_a) and (ξ_c, η_c). For the region 295 the curves are quite similar due to the proximity of the two origins; whereas in the region 276, in which the two origins are relatively more displaced, they are so different that they can be hardly recognised as belonging to the same region.

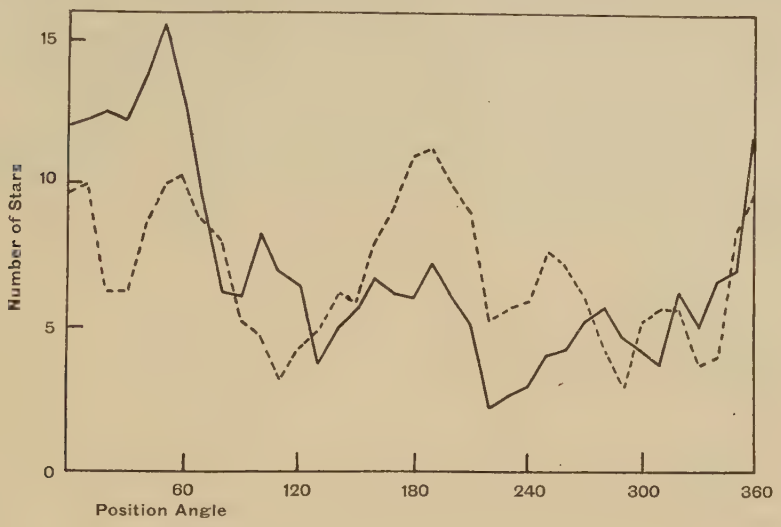

FIG. 2A.—*Frequency curves for region 276.*

Absolute origin (ξ_a, η_a); *curve* ————
Absolute origin (ξ_c, η_c); *curve* – – – – – –

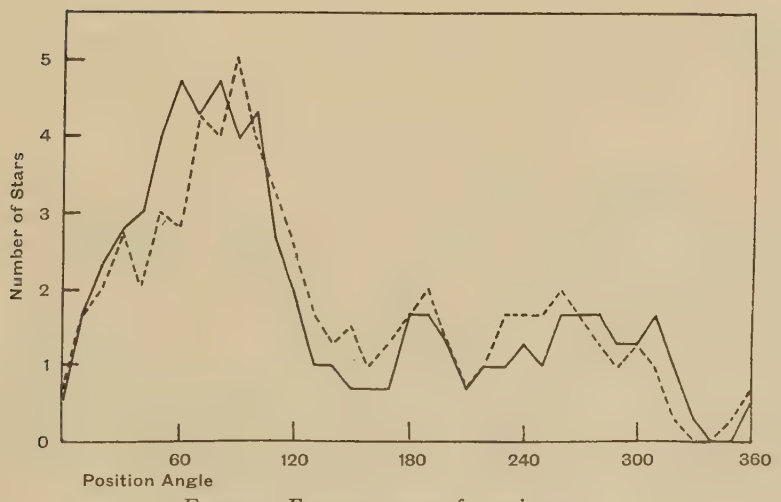

FIG. 2B.—*Frequency curves for region 295.*

Absolute origin (ξ_a, η_a); *curve* ————
Absolute origin (ξ_c, η_c); *curve* – – – – – –

Generally speaking, the frequency curves are distorted by considerable irregularities. A comparison with the frequency curves of the Cape Photographic Proper Motions as published by Smart and Tannahill * brings out this clearly. It is rather difficult therefore to analyse the curves by means of Eddington's "trial and error" method.

* Smart and Tannahill, *M.N.*, 100, 30, 1939.

In fact, the absolute origin seems to be indeterminate, indicating the presence of systematic or relatively larger accidental errors than have been estimated.

4. In order to find the presence of any systematic errors, I have followed Stenquist * by plotting μ_g (proper motion in galactic latitude) against the distance d, in mm., from the centre of the plate for all the B- and A-type stars ($m \geqslant 10^{m}\cdot0$) in the galactic regions 1, 8, 11, 79, 85 and 257 where these stars are comparatively more abundant. These faint stars were selected because their systematic motions perpendicular to the galactic place would, presumably, be negligible. Two kinds of systematic errors are thus revealed, of which the first is local to two or three regions only.

(1) In the two regions 79 and 85, and possibly in region 1 also, the dispersion in μ_g increases suddenly at about $d = 60$ mm. Fig. 3 shows this abrupt increase for the

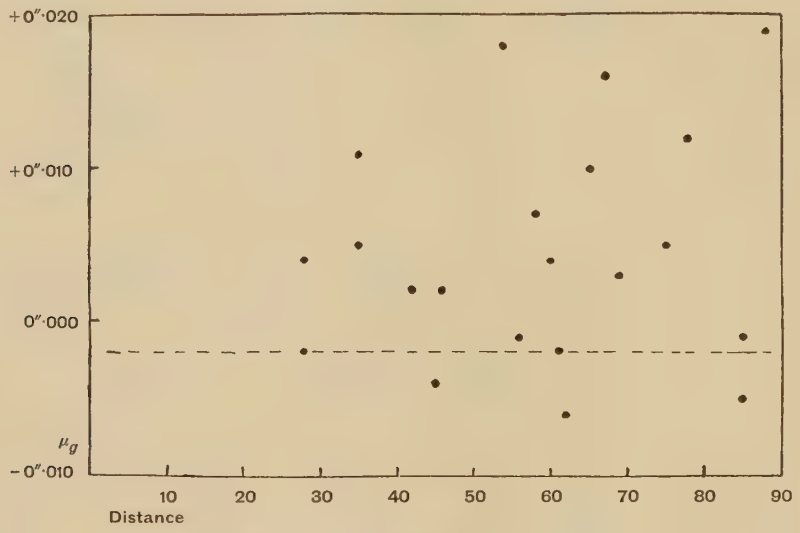

FIG. 3.—*Distribution of μ_g at different distances in mm. from the centre of the region 79.*

region 79. The absence of the proper motions near the centre is due to the use of the rotating sector. The figure shows clearly that the accuracy in proper motions falls off rather steeply beyond a certain distance from the centre. This defect is peculiar, however, to these two or three regions only and is not common to all.

(2) Removing the solar motion in galactic latitude ($-0''\cdot002$), we have only the peculiar motions perpendicular to the galactic plane. If these motions are purely random, they should be as many times positive as negative. In all except the last region, 257, so investigated, there is a strong preponderance of positive motions. This is shown in fig. 3 for the region 79 only, where the solar motion of $-0''\cdot002$ is shown by the broken line. For the region 257, the peculiar μ_g's are more negative. All the six regions thus show the common existence of some systematic error. As all the six regions are fairly widely distributed along the galactic equator, it is quite possible that this systematic error exists in all the galactic regions of this Publication. Perhaps it is this error which vitiates the distributions of the proper motions in position angle and distorts the frequency curves.

Summary

The distributions of McCormick proper motions in position angle for three groups are examined by assuming three "absolute" origins for each region. It is found that

* Stenquist, *Upsala Medd.*, No. 72, 59, 1937.

the frequency curves so obtained are very sensitive to the position of the absolute origin and that they vary very much from region to region for the same group. Although the two streams are on the whole shown, their analysis is heavily handicapped by the indeterminacy of the absolute origin. It is also established that in six galactic regions a common systematic error exists. In view of the fairly wide distribution of these regions, it is possible that this error may be common to all the galactic regions in the McCormick Publication.

University Observatory,
Glasgow, W. 2:
1941 *July* 2.

SOLAR MOTION AND GALACTIC ROTATION FROM O- AND B-TYPE STARS

A. Ali, M.A., B.Sc.

(Communicated by the Director, University Observatory, Glasgow)

(Received 1941 September 5)

Recently several papers have been published on the differential galactic rotation which account for the variation of the rotational constant, A, by introducing a mean coefficient of absorption in order to allow for the effects of interstellar matter on the distances of the stars. The absorption is determined by the usual "trial and error" methods so as to make A constant throughout a range of stellar distances. The present paper is an attempt to utilise in this direction the observational material published by Stebbins, Huffer and Whitford * on the colours of the B-type stars. Solar motion is also included in order to set at rest for good the status of the K term, which has been the subject of discussion since the publication of the work of Plaskett and Pearce on the motions of O- and B-type stars †, and this is made still more necessary by the investigation of Smart on the Scorpio-Centaurus Cluster.‡ We shall analyse here both the radial velocities and proper motions; the former for the K term, solar motion, Oort's first rotational constant, A, and the direction to the centre; the latter for the determination of the precessional errors and Oort's second rotational constant, B.

The radial velocities of the O- and B-type stars employed in this investigation were taken from the *General Catalogue of Radial Velocities of Stars, Nebulæ and Clusters*, by J. H. Moore.§ Some recently published velocities were also added to the Card Catalogue. The velocities of the spectroscopic binaries were obtained from the *Fourth Catalogue of Spectroscopic Binary Stars*, by J. H. Moore.‖ All the velocities are on the Lick system of radial velocities, while the spectral types are based on the system of Victoria classification of revised types.

The following stars were excluded: (1) Stars of B8 and B9 types; (2) stars beyond the galactic latitudes $\pm 25°$; (3) stars with less than three observations; (4) stars with the probable errors of radial velocities greater than 5 km./sec.; (5) stars with peculiar radial velocities, *i.e.* greater than 45 km./sec., after correction for normal solar motion; (6) members of open clusters (h and χ Persei, Pleiades and Perseus). The members of h and χ Persei and Pleiades were identified by means of the lists given by van Maanen ¶ and Rasmuson.** Several Perseus stars whose membership of the cluster is considered quite probable by Smart and Ali †† were also excluded.

After all these rejections, there were 788 stars of O- and B-type with reliable radial velocities in the Card Catalogue.

1. *Photometric Distances and Space Absorption.*—In order to analyse the radial velocities for the differential galactic rotation, it is necessary to divide the total number of stars into distance groups. For this purpose, the trigonometrical parallaxes are of little use as they are scarcely to be had for the early types, and the spectroscopic parallaxes are only available for the bright stars; besides, the necessity of correcting the distances for the space absorption still remains. Hence the following procedure was adopted.

As the dispersion in the absolute magnitudes of the early types is small, we can use

* *Ap. J.*, 91, 20, 1940. † *Pub. D.A.O.*, 5, part 4, 1936. ‡ *M.N.*, 100, 60, 1939.
§ *Lick Pub.*, 18, 1932. ‖ *Lick Bull.*, 18, 1, 1936. ¶ *Mt. Wilson Contr.*, No. 205.
** *Lund Medd.*, Ser. II, No. 26, 1921. †† *M.N.*, 100, 560, 1940.

the following relation for determining the photometric distance r in parsecs defined by

$$M = m - \Delta m + 5 - 5 \log r, \qquad (1)$$

where M is the mean absolute magnitude of a star for a given spectral type, m its apparent visual magnitude and Δm the total visual absorption in magnitudes. Δm has been expressed by Stebbins, Huffer and Whitford * in terms of the photoelectric colour excess measured for 1332 B-type stars. They find that $\Delta m = 7E_1$ where E_1 is the photoelectric colour excess on their scale. Therefore substituting for Δm in (1), we get

$$\log r = 0{\cdot}2(m_0 - M) + 1, \qquad (2)$$

where $m_0 - M = (m - 7E_1) - M$ is the distance modulus corrected for the space absorption. The corrected distance moduli are given by Stebbins, Huffer and Whitford for about 1300 stars. Therefore r can be found from (2) for a star whose photoelectric colour excess, E_1, is known.

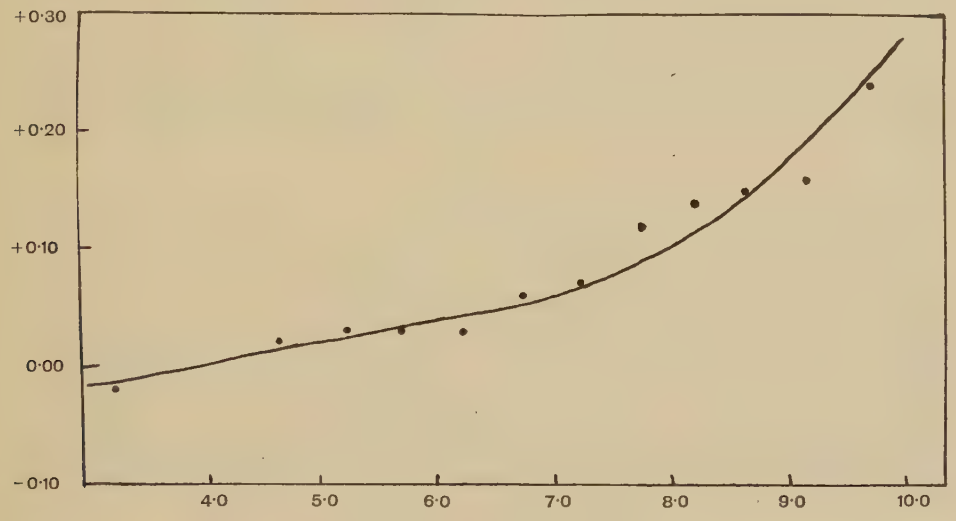

FIG. 1.—*Magnitude-colour excess diagram for the B3 type.*

Abscissa: magnitude (m). *Ordinate: photoelectric colour excess* (E_1).

When no photoelectric colour excesses were available, the following method was adopted. If the mean photoelectric colour excess (E_1) is plotted against the mean apparent visual magnitude (m) in a narrow magnitude range for a given spectral type, it is found that there is a strong correlation between m and E_1. A smooth curve can usually be drawn through the points (m, E_1) for each subtype or a narrow range of subtypes if the number of stars is small. From such a curve, E_1 can easily be read off for a given magnitude and type. One of the curves is shown in fig. 1 for the B3 type. The range in the magnitude for the stars with $m < 5^{m}{\cdot}0$ is $1^{m}{\cdot}0$ and for the stars with $m \geqslant 5^{m}{\cdot}0$ is $0^{m}{\cdot}5$. The subtypes B4 and B5, B6 and B7, were combined as the number of stars in some of these groups is rather small. In this way, for stars with no measured photoelectric colour excesses, "theoretical" colour excesses were obtained. The same absolute magnitudes given by Stebbins, Huffer and Whitford were employed for determining the corrected distance moduli ($m_0 - M$). This indirect procedure was necessary for 263 stars. It must be mentioned that the adopted absolute magnitudes are on the average about one magnitude brighter for the early B-type stars. They were determined by Stebbins, Huffer and Whitford † by combining the means of the absolute magnitudes

* *Loc. cit.* † *Loc. cit.*

derived by Plaskett and Pearce and by Strömberg after correcting for the estimated absorption of $7E_1$ with the independent solutions made from the radial velocities and from the close pairs of B-type stars with the same colour excess.

The stars were now divided into four distance groups according to $(m_0 - M)$ as shown in Table I. The mean distance $(\bar{r})$ is not corrected for the effect of dispersion of the absolute magnitudes about their mean, since this effect is more or less counterbalanced by the correlation between the absolute and fainter apparent magnitudes as shown by Nordstrom.*

TABLE I

Division into Distance Grouping

Distance Group	No. of Stars	$m_0 - M$	Mean Distance in Parsecs $(\bar{r})$
		m	
I	81	$\geqslant 9{\cdot}5$	1152
II	174	9·4–8·5	598
III	232	8·4–7·5	398
IV	301	$< 7{\cdot}5$	220

2. *Analysis of the Radial Velocities.*—The well-known equation of condition involving the solar motion, rotational term and the radial velocity, with the usual K term in km./sec., is

$$K + lX + mY + nZ + \bar{r}A \sin 2(G - G_0) \cos^2 g = V, \tag{3}$$

where l, m, n are the direction cosines of the radius vector joining the Sun and the star whose galactic longitude and latitude are (G, g), $(-X, -Y, -Z)$ are the rectangular components of the solar motion in km./sec. along the galactic axes, A Oort's rotational constant in km./sec./parsec, G_0 the galactic longitude of the centre and V the radial velocity of the star in km./sec. relative to the Sun. As the early-type stars are strongly concentrated towards the galactic plane, the Z component of the solar motion perpendicular to the galactic plane becomes indeterminate. It is therefore necessary to assume Z and eliminate it from (3). Assuming the standard solar apex $(G_\odot = 23^\circ{\cdot}5, g_\odot = +21^\circ{\cdot}6)$, and a solar velocity of 19·5 km./sec., Z is equivalent to $-7{\cdot}2$ km./sec. Hence the correction to the observed radial velocity is $+7{\cdot}2 \sin g$. The maximum value of this correction in our case is numerically 3 km./sec. Modifying accordingly and expanding (3), we have

$$K + lX + mY + pu + qv = V_1, \tag{4}$$

where the known quantities are $l = \cos G \cos g$, $m = \sin G \cos g$, $p = \sin 2G \cos^2 g$, $q = -\cos 2G \cos^2 g$ and $V_1 =$ the corrected radial velocity; the unknowns are $K =$ the K term $(-X, -Y) =$ the components of the solar motion in the galactic plane, $u = \bar{r}A \cos 2G_0$ and $v = \bar{r}A \sin 2G_0$, which give after solving

$$\left.\begin{aligned} S_G &= \text{solar velocity in the galactic plane} = (X^2 + Y^2)^{\frac{1}{2}}, \\ G_\odot &= \text{galactic longitude of the solar apex} = \tan^{-1}\left(\frac{Y}{X}\right), \\ \bar{r}A &= \text{amplitude of the rotational term} = +(u^2 + v^2)^{\frac{1}{2}}, \\ G_0 &= \text{galactic longitude of the centre} = \tfrac{1}{2}\tan^{-1}\left(\frac{v}{u}\right). \end{aligned}\right\} \tag{5}$$

Equation (4) is our fundamental equation of condition when applied to each of the four distance groups; it means that we are practically solving for twenty unknowns. If, on the other hand, we assume a common K term and solar motion for all the early-type stars, then a general equation of eleven unknowns can be written for the four distance groups. Both the equation (4) and the general equation were applied to the radial

* *Lund Medd.*, Ser. II, No. 79, 1936.

velocity data of the four distance groups; the corresponding results have been termed individual and general solutions respectively. The normal equations for the general equation were formed by the appropriate combinations of the four sets of the normal equations of the individual distance groups.

In order to facilitate the application of the equation of condition (4), each of the four distance groups was divided into longitude groups, the range in longitude being about 15°. In forming these subgroups, the grouping tendencies of these stars were, whenever possible, kept in mind. In each longitude group, the means of l, m, p, q and V_1 were formed instead of referring the mean of V_1 to the geometrical centre of the subgroup, and the weight assigned to a subgroup was equal to the number of the stars in it. The results of the individual and general solutions are given separately for the solar motion and galactic rotation in Tables II and III with the probable errors. The values given in these tables were obtained by means of equations (5).

3. *The K Term and Solar Motion.*—In Table II the successive columns indicate the distance groups with the number of stars in the group in brackets, the mean distance of the group ($\bar{r}$) in parsecs, the K term in km./sec., the galactic longitude of the solar apex $G_\odot$, the solar velocity in the galactic plane S_G in km./sec., and finally the solar velocity S in km./sec. by assuming the Z component of the solar motion to be $-7{\cdot}2$ km./sec. The second lines in the distance groups I, II and III show the various values when the K term is assumed zero. The last lines give the values derived from the general equation.

TABLE II

The K Term and Solar Motion

Distance Group	$\bar{r}$	K	$G_\odot$	S_G	S
			° °		
I (81)	1152	$+1{\cdot}52 \pm 3{\cdot}11$	$36{\cdot}7 \pm 17{\cdot}4$	$13{\cdot}89 \pm 4{\cdot}22$	15·64
		(0)	$28{\cdot}8 \pm 10{\cdot}9$	$11{\cdot}92 \pm 2{\cdot}26$	13·92
II (174)	598	$-0{\cdot}76 \pm 0{\cdot}83$	$9{\cdot}4 \pm 6{\cdot}1$	$15{\cdot}05 \pm 1{\cdot}61$	16·65
		(0)	$11{\cdot}9 \pm 5{\cdot}4$	$15{\cdot}11 \pm 1{\cdot}42$	16·74
III (232)	398	$-0{\cdot}74 \pm 0{\cdot}60$	$18{\cdot}4 \pm 2{\cdot}5$	$18{\cdot}54 \pm 0{\cdot}81$	19·89
		(0)	$17{\cdot}5 \pm 2{\cdot}4$	$18{\cdot}38 \pm 0{\cdot}77$	19·74
IV (301)	220	$+3{\cdot}63 \pm 0{\cdot}44$	$31{\cdot}2 \pm 1{\cdot}8$	$20{\cdot}89 \pm 0{\cdot}64$	22·10
General Solution (788)	...	$+2{\cdot}17 \pm 0{\cdot}40$	$28{\cdot}6 \pm 1{\cdot}8$	$18{\cdot}73 \pm 0{\cdot}58$	20·07

The third column in Table II shows that, in each of the first three relatively more distant groups, the probable errors of the K term are (if not greater) of the same magnitude as the K term itself. Putting $K = 0$ does not materially improve the values of $G_\odot$ and S_G for the three groups. This means that either the K term does not exist for the B-type stars in the more distant groups, or the considerable uncertainties in the values of $G_\odot$ and S_G conceal it. On the other hand, the fourth group, the nearest one, yields a real K term of $+3{\cdot}63 \pm 0{\cdot}44$ km./sec.

The solar motion for the two distance groups I and II is rather indeterminate. The considerable uncertainty in the longitude of the solar apex ($36°{\cdot}7 \pm 17°{\cdot}4$ and $9°{\cdot}1 \pm 6°{\cdot}1$) with the corresponding uncertainty of the solar velocity in the galactic plane, may be ascribed to the fact that the number of stars in the two groups is too small to eliminate properly the effects of the peculiar motions. It must be mentioned that the distribution of the stars in group I along the galactic circle is not uniform, there being a big gap between longitudes about 190° and 320° which is probably responsible for the sudden drop in the probable errors of group I when K is assumed zero. The average residuals (unit weight) without regard to signs are 11·7 and 10·9 km./sec. for groups I and II.

Group III gives practically a normal solar motion with a solar speed of 19·89 km./sec. and longitude of the solar apex 18°·4 ± 2°·5, about 5° off the standard apex. In group IV, the nearest group, we find that the solar speed and the longitude of the solar apex have appreciably increased to 22·10 km./sec. and 31°·2 ± 1°·8 compared with their values in the third group. The average residuals (unit weight) without regard to signs are 8·1 and 8·6 km./sec. for the groups III and IV. Only in the third group the residuals (unit weight) show a tendency to be periodic with respect to the longitude of the subgroups.

The apparent variation of the solar motion vector for the relatively more distant groups cannot be accepted with confidence in view of the rather large uncertainty attached to it. It seems therefore best to assume that this vector does not vary in the different volumes of space in the neighbourhood of the Sun for the early-type stars and that a common K term characterises it. The general solution, which is based upon these assumptions, gives a K term of +2·17 ± 0·40 km./sec., a solar speed of 20·07 km./sec. and the longitude of the solar apex 28°·6 ± 1°·8, which is about 5° off the standard solar apex. The most noteworthy fact about the general solution is that it gives not only an almost normal solar motion, but also yields a very much reduced K term which is comparable with the gravitational shift of the spectral lines for these stars. This shift as determined from the data of the *Fourth Catalogue of Spectroscopic Binary Stars* for the early types (revised types only) amounts to about +1·6 km./sec. It will thus be seen that the general solution value of the K term is of the same order as the gravitational shift. The conclusion reached here is the same as that of Plaskett and Pearce * but is less open to the objections raised against them.†

We conclude therefore from the analysis of the radial velocities of the early-type stars that the solar motion when referred to the totality of these stars is not very much off the normal standard, and that the K term can be identified with the gravitational shift towards the red in the spectral lines of these massive stars.

4. *The Rotational Constant A and the Longitude of the Centre, G_0.*—Table III gives the values of the amplitude of the rotational term $\bar{r}A$ in km./sec., the longitude of the centre, G_0, and the derived values of A in km./sec./parsec with the probable errors both for the individual and general solutions. The probable errors attached to A do not take cognisance of any errors in $\bar{r}$. The values of these constants when the K term is assumed zero for groups I, II and III in the individual solutions are not given as they are not of much interest.

TABLE III

The Rotational Constant A and the Longitude of the Centre

Distance Group	$\bar{r}$	Individual Solution			General Solution		
		$\bar{r}A$	G_0	A	$\bar{r}A$	G_0	A
I (81)	1152	+18·50 ± 3·40	319°·2 ± 5°·3	+0·0161 ± 29	+17·39 ± 1·70	324°·5 ± 2°·8	+0·0151 ± 15
II (174)	598	+ 8·68 ± 1·55	310·6 ± 5·1	+0·0145 ± 26	+ 6·78 ± 1·22	319·4 ± 5·1	+0·0113 ± 20
III (232)	398	+ 5·08 ± 0·81	320·6 ± 4·6	+0·0128 ± 20	+ 4·27 ± 1·03	311·9 ± 6·9	+0·0107 ± 26
IV (301)	220	+ 1·91 ± 0·66	286·2 ± 9·9	+0·0087 ± 30	+ 1·30 ± 0·91	278·7 ± 20·1	+0·0059 ± 41

The interesting thing about Table III is that A diminishes with decreasing $\bar{r}$ in both solutions. How far this trend is real cannot be judged on account of the fact that the

* *Loc. cit.*

† See Smart, *M.N.*, **96**, 568, 1936; **100**, 370, 1940.

probable errors of A do not take into account the errors in $\bar{r}$. Again, the same trend is shown for G_0 in the general solution; but here the probable errors of G_0 also increase at the same time, indicating that the trend here is not real. Finally the values of A and G_0 for the nearest group (group IV) are very distorted. This is to be expected, as the value of the rotational term involved is of the order of 3 km./sec. for this group.

Combining the four values of A in both solutions, we get the following weighted mean values:—

$$A = +0.0131 \pm 0.0013 \text{ km./sec./parsec (individual solution)}$$
$$= +0.0127 \pm 0.0010 \text{ km./sec./parsec (general solution).}$$

There is not much difference in two sets of the above values of A. The general solution value is, however, adopted as definitive. Two recent studies of differential rotation by Joy * and Wilson † give a larger value of A ($+0.0209 \pm 0.0008$ km./sec./parsec and $+0.0177 \pm 0.0007$ km./sec./parsec respectively). The discrepancy between my value of A and those of Joy and Wilson is rather unexpected, as in each case absorption in one way or another has been considered.

The longitudes of the direction to the centre as determined from the general solution are in satisfactory agreement with the direction given by Shapley ‡ from the study of the distribution of the globular clusters. The weighted mean values are:

$$G_0 = 314^\circ.6 \pm 2^\circ.8 \text{ (individual solution)}$$
$$= 321^\circ.5 \pm 2^\circ.3 \text{ (general solution).}$$

The individual solution value is about 10° off the usually accepted figure of 325°. The definitive value has been taken as $G_0 = 321^\circ.5 \pm 2^\circ.3$.

5. *Analysis of the Proper Motions.*—Out of a total of 788 stars whose radial velocities have been analysed above, there are 705 stars whose proper motions can be obtained from the new *General Catalogue* published by the Carnegie Institute of Washington. In order to determine the precessional corrections and the second rotational constant B, the proper motions are taken within a narrower zone of $\pm 20^\circ$ in galactic latitude. Excluding thus 34 stars with latitudes beyond $\pm 20^\circ$ and 3 stars with centennial probable errors of proper motions greater than $1''.49$, there are 668 stars whose proper motions have been analysed. The assigned weights (scheme A) according to the centennial probable errors are as follows: $< 0''.50$, weight 3; $0''.50 - 0''.99$, weight 2; $1''.00 - 1''.49$, weight 1; $> 1''.49$, weight 0. In order to avoid overweighting the more populated subgroups, the adopted weights (scheme B) that were applied to each subgroup are based on its total weight as determined from scheme A. These adopted weights are given below:

Total weight (scheme A)	1 – 3,	4 – 9,	10 – 39,	⩾ 40.
Adopted weight (scheme B)	½ ,	1,	2,	3.

No proper motions were rejected on account of their large magnitude.

Before determining the second rotational constant B, we require to eliminate from the observed proper motions the effects of the parallactic motion and the systematic motion due to the errors of the adopted precessional constants. The parallactic components in the equatorial co-ordinates were obtained for each star by employing an assumed solar apex (18^h, $+31^\circ$) with the solar velocity of 20 km./sec. (as given by the general solution of the radial velocities) and the star's parallax as determined by the photometric distance. Removing these from the observed proper motions ($\mu_\alpha \cos\delta$, μ_δ) in the equatorial co-ordinates, we have the peculiar proper motions (ξ, η) in seconds of arc per annum in the equatorial system. In order to determine the precessional errors from the equation of condition (6) below, the peculiar motions (ξ, η) were converted into the component of proper motion in galactic latitude (μ'_g).

* *Ap. J.*, **89**, 356, 1939. † *Ap. J.*, **92**, 170, 1940. ‡ *Star Clusters*, p. 22, 1930.

6. *Corrections for the Precessional Errors.*—It can be shown that for a star (galactic longitude G) near the galactic plane, if any systematic motions perpendicular to the galactic plane are regarded as negligible,

$$\mu'_g = x \cos G + y \sin G, \tag{6}$$

where

$$x = (+0{\cdot}086\Delta n - 0{\cdot}885\Delta k), \qquad y = +0{\cdot}985\Delta n, \tag{7}$$

and Δk and Δn are the corrections to the adopted precessional constants in right ascension and declination respectively.

The observational data in each of the four distance groups was divided into subgroups, each group covering a range of 20° in longitude. The means of μ_g', cos G and sin G were formed and the equation of condition (6) was then applied. The least-squares solutions give the following values of x and y with their probable errors (Table IV):—

TABLE IV

The Precessional Errors

Distance Group	x	y
	″ ″	″ ″
I	−0·0014 ±0·0014	−0·0002 ±0·0014
II	+0·0027 ±0·0010	+0·0067 ±0·0010
III	+0·0032 ±0·0009	+0·0029 ±0·0009
IV	+0·0019 ±0·0011	+0·0056 ±0·0006
Combined (*a*)	+0·0021 ±0·0005	+0·0044 ±0·0005
Combined (*b*)	+0·0017 ±0·0006	+0·0052 ±0·0006

Except for the first group (where the number of stars is too small), the values of x and y are fairly satisfactory. Combining the four groups we get the solution, combined (*a*), in Table IV. This gives by means of equations (7)

$$\Delta k = -0''{\cdot}0019 \pm 0''{\cdot}0006,$$
$$\Delta n = +0''{\cdot}0045 \pm 0''{\cdot}0005.$$

However, if we solve (6) for all the 668 stars without any regard to the distance grouping and modify accordingly the adopted weights (scheme B), we get the solution, combined (*b*), which gives

$$\Delta k = -0''{\cdot}0014 \pm 0''{\cdot}0007,$$
$$\Delta n = +0''{\cdot}0053 \pm 0''{\cdot}0006.$$

Taking the simple means of the above two sets as the definitive values and attaching the probable errors of the second set, we have

$$\Delta k = -0''{\cdot}0017 \pm 0''{\cdot}0007,$$
$$\Delta n = +0''{\cdot}0049 \pm 0''{\cdot}0006.$$

Hence the corrections to be applied to the equatorial components of the annual proper motions of the new *General Catalogue* are

$$\left.\begin{aligned} \Delta\mu_\alpha \cos\delta &= +0''{\cdot}0017 \cos\delta - 0''{\cdot}0049 \sin\alpha \sin\delta, \\ \Delta\mu_\delta &= -0''{\cdot}0049 \cos\alpha. \end{aligned}\right\} \tag{8}$$

Fig. 2 shows the distribution of the mean peculiar proper motion in galactic latitude, $\bar{\mu}_g'$, with respect to the galactic longitude. The theoretical curve

$$\bar{\mu}_g' = +0''{\cdot}0019 \cos G + 0''{\cdot}0048 \sin G$$

is shown by the thick line and the observed values of $\bar{\mu}_g'$ by dots. The numerical coefficients in the theoretical curve are the means of the two values of x and y in the combined solutions (*a*) and (*b*).

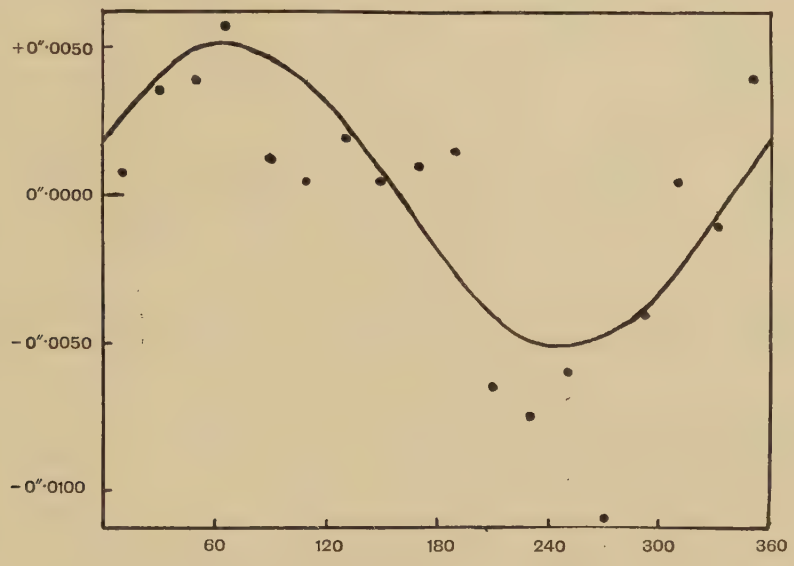

FIG. 2.—*Distribution of $\bar{\mu}_g'$ in galactic longitude.*

Abscissa: galactic longitude. Ordinate: $\bar{\mu}_g'$.

7. *The Second Rotational Constant, B.*—The equation of condition involving $\mu_G' \cos g$, the two rotational constants A and B in km./sec./parsec and the galactic longitude of the centre G_0 is

$$\mu_G' \cos g = \frac{A}{4{\cdot}74} \cos 2(G - G_0) \cos g + \frac{B}{4{\cdot}74} \cos g, \qquad (9)$$

where $\mu_G' \cos g$ is the component of proper motion in galactic longitude of a star with co-ordinates G, g. $\mu_G' \cos g$ was obtained after applying the corrections for the precessional errors by means of equations (8) and for the parallactic motion to the observed proper motions ($\mu_\alpha \cos \delta$, μ_δ) in the equatorial co-ordinates. Equation (9) was applied to the observational data in two ways: (1) by solving for the three unknowns G_0, $\frac{A}{4{\cdot}74}$ and $\frac{B}{4{\cdot}74}$; and (2) by solving for one unknown, $\frac{B}{4{\cdot}74}$, only, by substituting in (9) the definitive values of A and G_0 derived in the radial velocity analysis. Further, the distance grouping, though unnecessary, was modified by combining groups I and II. Each of the three distance groups was now divided into eighteen longitude groups, each covering a range of 20° in longitude. Equation (9) was of course applied to the means of the known quantities in each subgroup.

The results of the least-squares solutions are given in Table V with the probable errors. The first three columns give the values when the equation (9) is solved for the three unknowns G_0, $\frac{A}{4{\cdot}74}$ and $\frac{B}{4{\cdot}74}$. The last column is obtained by solving for $\frac{B}{4{\cdot}74}$ only as indicated above. The last line gives the values of the unknowns when the three groups are combined. The values of G_0 and $\frac{A}{4{\cdot}74}$ in the now distant group (I + II) are rather unexpectedly in good agreement with the usual values obtained from the

TABLE V

The Rotational Constants from the Proper Motions

Distance Group	G_0	$\frac{A}{4{\cdot}74}$	$\frac{B}{4{\cdot}74}$ Method (i)	$\frac{B}{4{\cdot}74}$ Method (ii)
	° °	″ ″	″ ″	″ ″
(I + II)	327·0 ± 7·5	+0·0038 ± 0·0010	−0·0033 ± 0·0007	−0·0032 ± 0·0007
III	296·2 ± 21·6	+0·0016 ± 0·0012	−0·0049 ± 0·0008	−0·0043 ± 0·0008
IV	312·4 ± 33·8	+0·0011 ± 0·0013	−0·0044 ± 0·0008	−0·0043 ± 0·0007
Combined	333·4 ± 12·3	+0·0014 ± 0·0006	−0·0041 ± 0·0004	−0·0040 ± 0·0005

radial velocities; the values of these constants in the other two groups and the combined solution are obtained, however, with rather low weight. On the other hand, the values of $\frac{B}{4{\cdot}74}$ are derived with greater accuracy in both solutions, and they are also in satisfactory agreement with each other. There is, however, little to choose between the two sets of the values for $\frac{B}{4{\cdot}74}$. The combined solution value $\frac{B}{4{\cdot}74} = -0''{\cdot}0040 \pm 0''{\cdot}0005$ when A and G_0 have been assumed has been adopted as definitive. It must be mentioned that the probable error attached to the definitive value of $\frac{B}{4{\cdot}74}$ does not take into account the errors inherent in the corrections for the precessional errors that have been applied differentially to the observed proper motions.

Wilson and Raymond * have recently obtained this constant from all the G.C. stars as $-0''{\cdot}0025 \pm 0''{\cdot}0003$, and from 1591 B-type stars, $-0''{\cdot}0041 \pm 0''{\cdot}0008$. The latter value agrees quite well with the definitive value derived above in spite of the different method of treatment and the different number of stars involved. The anomalous behaviour of this constant when determined from the stars all over the sky and from the stars concentrated near the galaxy remains unexplained.

Fig. 3 shows the mean proper motions, $\bar{\mu}_G'$, in the galactic equator plotted against the galactic longitude. The proper motions, $\bar{\mu}_G'$, have been corrected for the solar motion and precessional errors as outlined above. The theoretical curve

$$\bar{\mu}_G' = +0''{\cdot}0027 \cos 2(G - 321°{\cdot}5) - 0''{\cdot}0040$$

is shown by the thick line in the figure. The constants in this equation are the definitive values of $\frac{A}{4{\cdot}74}$, G_0 and $\frac{B}{4{\cdot}74}$. The dots refer to the weighted mean values of $\bar{\mu}_G'$ in the three distance groups. The figure shows that there are still some systematic deviations in certain intervals of longitude, especially about the region near 250° and between 280° and 320°.

8. *Some Dynamical Consequences.*—With the values of $\frac{A}{4{\cdot}74} = +0''{\cdot}0027$ and $\frac{B}{4{\cdot}74} = -0''{\cdot}0040$, we get the angular velocity of rotation in the neighbourhood of the Sun $\omega = 0''{\cdot}0067$ per annum, which gives the period of rotation at the Sun $P = 1{\cdot}9 \times 10^8$ years. Assuming 275 km./sec. as the rotational velocity of the Sun, the distance to the centre is about 8700 parsecs.

* *Ap. J.*, 47, 49, 1938.

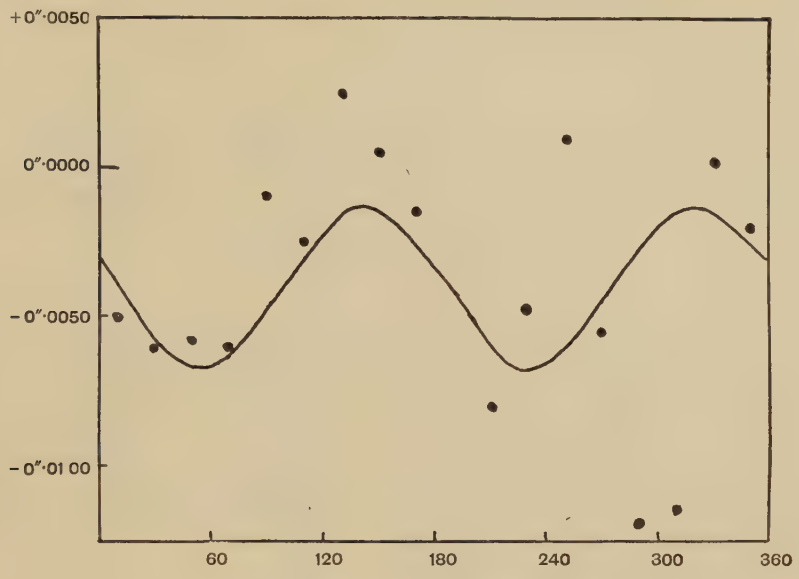

FIG. 3.—*Distribution of $\bar{\mu}_G'$ in galactic longitude.*

Abscissa: galactic longitude. Ordinate: $\bar{\mu}_G'$.

Summary

The radial velocities of 788 early-type stars have been analysed for the K term, solar motion and galactic rotation. The stars were divided into four distance groups, taking into account the space absorption based on observational data. When solved for the individual distance groups, the K term does not seem to exist for the three relatively more distant groups but emerges with a value of $+3{\cdot}63 \pm 0{\cdot}44$ km./sec. in the nearest group. Assuming, however, that the solar motion vector is constant for the early-type stars in the different volumes of space surrounding the Sun and that a common K term characterises it, we get a K term of $+2{\cdot}17 \pm 0{\cdot}40$ km./sec. with the solar velocity 20·07 km./sec. in the direction of $28°{\cdot}6 \pm 1°{\cdot}8$ in the galactic equator. This value of the K term is of the same order as the gravitational shift of the spectral lines towards the red, which is equivalent to about + 1·6 km./sec. for these massive stars and can therefore be identified with it. The weighted mean value of the rotational constant is $+0{\cdot}0127 \pm 0{\cdot}0010$ km./sec./parsec and that of the longitude of the centre is $321°{\cdot}5 \pm 2°{\cdot}3$. From the analysis of the proper motions, the correction for the precessional errors in right ascension and declination are $\Delta k = -0''{\cdot}0017 \pm 0''{\cdot}0007$, $\Delta n = +0''{\cdot}0049 \pm 0''{\cdot}0006$. The second rotational constant is $\frac{B}{4{\cdot}74} = -0''{\cdot}0040 \pm 0''{\cdot}0005$. The corresponding angular velocity in the neighbourhood of the Sun is $\omega = 0''{\cdot}0067$, which gives the period of rotation $1{\cdot}9 \times 10^8$ years. The distance to the centre is about 8700 parsecs.

In conclusion, I wish to express my warm gratitude to Professor W. M. Smart, Regius Professor of Astronomy in the University of Glasgow, for his interest and guidance throughout the course of the present investigation, and also to Professor Sir Arthur Eddington for a valuable discussion over the subject-matter of the present paper during my stay at Cambridge.

University Observatory,
Glasgow, W. 2:
1941 *September* 5.

POSITIONS OF COMETS DETERMINED AT THE ROYAL OBSERVATORY, CAPE OF GOOD HOPE, 1941 JANUARY–JUNE

(Communicated by H.M. Astronomer)

(Received 1941 August 25)

The following positions were derived from photographs taken with the astrographic telescope. The telescope was guided on stars, so that for the longer exposures, especially of Van Gent's Comet, there was some trailing of the comet. The comet has generally been measured against four comparison stars within 40′ of it. The star places were adapted from the best catalogues available and reduced to 1941·0 with proper motions when known. For Cunningham's Comet the stars were all taken from the Cape Zone Catalogue for 1900·0, $-40°$ to $-52°$, with photographic proper motions. For de Kock's Comet the star places used were as follows:—

Jan.	20–22	General Catalogue (Albany)
	23–25	Cape Zone Catalogue
	26	General Catalogue
	27–28	La Plata Catalogues A and B, and General Catalogue
Feb.	2	Unpublished Cape Catalogue on FK3 system
	4	General Catalogue
	7	Yale Photographic Catalogue
	9	General Catalogue
	14–27	A.G. Catalogues and Pulkova Catalogues reduced to G.C. system
Mar.	6	A.G. and General Catalogue

The star places for the later observations, especially for February 14, were not very satisfactory.

For Van Gent's Comet the star places of the first night were from Cordoba A, for the second night from the General Catalogue and for the third night from the Albany A.G. Catalogue.

The positions given require corrections for

(1) Aberration due to the Earth's motion.
(2) The time taken by light in passing from the comet to the Earth.
(3) Parallax.

The last correction is obtained by dividing the quantities tabulated by the distance of the comet.

Nearly all the plates were taken with the comets low in the sky. Towards the end Comet Cunningham was better placed, but when the first plate of it was taken the altitude was less than 11°. On account of the quality of the images it was not thought necessary to apply corrections for second-order terms in differential refraction.

De Kock's Comet

Date	U.T.	R.A. (1941·0)	Dec.	Parallax × Distance		Exposure
	d	h m s	° ′ ″	s	″	s
1941 Jan.	20·12149	16 07 06·32	−39 21 01·2	−·548	−1·50	15
	·12230	06·84	06·5	−·547	−1·47	5
	·12253	06·98	08·0	−·546	−1·47	5
	·12340	07·32	13·8	−·545	−1·45	15
	21·11193	16 17 08·71	−41 19 00·0	−·590	−1·66	60
	·11441	10·40	17·7	−·586	−1·60	30
	·11544	11·00	25·5	−·584	−1·57	30
	22·10745	16 29 49·80	−43 32 42·0	−·629	−1·76	60
	·10867	50·86	53·0	−·627	−1·72	30
	·10910	51·11	57·7	−·626	−1·71	15
	·10945	51·42	−43 33 00·2	−·626	−1·70	15
	23·12021	16 46 27·17	−46 04 52·2	−·651	−1·40	60
	·12125	28·21	05 02·6	−·649	−1·37	30
	·12201	29·07	10·0	−·648	−1·35	30
	·12264	29·80	15·7	−·646	−1·33	30
	24·11733	17 07 56·90	−48 48 45·6	−·709	−1·63	5
	·11803	57·96	53·6	−·708	−1·61	5
	·11872	59·88	−48 49 00·2	−·707	−1·59	5
	25·12752	17 37 01·84	−51 42 02·0	−·763	−1·63	15
	·12784	02·47	05·7	−·762	−1·61	10
	·12805	02·75	07·0	−·762	−1·61	5
	·12839	03·55	12·2	−·761	−1·60	5
	26·12514	18 15 35·60	−54 23 45·6	−·834	−2·36	9
	·12552	36·54	50·6	−·834	−2·34	5
	·12607	38·12	54·4	−·834	−2·32	5
	·12630	38·55	56·4	−·834	−2·32	5
	27·11690	19 05 47·64	−56 23 35·8	−·867	−3·76	60
	28·12681	20 08 05·94	−56 56 38·0	−·834	−4·86	30
	·12794	10·19	37·7	−·837	−4·82	15
	·12829	11·69	38·2	−·837	−4·81	15
	·12860	12·82	36·7	−·838	−4·79	10
1941 Feb.	2·80742	0 18 58·08	−31 00 36·5	+·554	−3·34	5
	·80765	58·44	33·2	+·554	−3·35	5
	4·80763	0 48 59·83	−21 59 48·8	+·498	−3·66	30
	·80801	0 49 00·09	42·8	+·499	−3·67	5
	·80818	00·26	41·0	+·499	−3·67	5
	7·79743	1 14 30·89	−12 45 00·6	+·451	−4·06	60
	·79812	31·21	−12 44 54·2	+·452	−4·07	30
	·79863	31·42	49·3	+·452	−4·08	30
	9·79324	1 24 57·35	− 8 32 32·4	+·436	−4·32	10
	·79364	57·39	29·0	+·437	−4·33	20
	·79405	57·46	26·2	+·437	−4·33	30
	14·78124	1 40 22·00	− 1 49 33·1	+·418	−4·76	120
	·78245	22·15	28·8	+·420	−4·76	60
	·78315	22·30	26·7	+·421	−4·76	30
	22·77223	1 50 50·32	+ 3 41 58·3	+·427	−5·11	120
	·77343	50·35	42 00·3	+·429	−5·11	60
	·77430	50·45	02·0	+·430	−5·10	60
	25·77368	1 54 24·49	+ 5 00 34·4	+·438	−5·15	60
	·77453	24·48	36·2	+·439	−5·15	60
	·77777	24·69	42·9	+·444	−5·14	180
	27·76573	1 55 50·80	+ 5 44 51·6	+·434	−5·20	120
	·76942	51·05	56·8	+·439	−5·18	120
1941 Mar.	6·75863	1 59 51·02	+ 7 46 33·4	+·448	−5·25	300
	·76187	51·01	36·1	+·452	−5·23	180

Cunningham's Comet

Date	U.T.	R.A. (1941·0)	Dec.	Parallax × Distance		Exposure
	d	h m s	° ′ ″	s	″	s
1941 Jan.	25·11769	19 32 38·54	−43 07 09·1	−·634	−5·14	180
	·11934	38·60	12·8	−·636	−5·09	15
	·11968	38·84	12·4	−·636	−5·08	15
	·12003	38·88	14·2	−·637	−5·07	15
	·12326	39·02	22·5	−·641	−4·97	60
	26·11676	19 34 34·46	−43 42 44·7	−·641	−5·10	300
	·12015	34·81	51·3	−·645	−5·00	30
	·12065	34·75	53·0	−·646	−4·98	15
	·12105	35·02	52·7	−·646	−4·97	16
	28·11157	19 38 48·82	−44 35 56·5	−·647	−5·16	300
	·11520	49·19	−44 36 02·1	−·652	−5·15	60
	·11590	49·20	02·0	−·653	−5·02	30
	·11642	49·43	04·0	−·653	−5·01	30
1941 Feb.	3·11073	19 52 56·88	−45 43 43·6	−·668	−4·94	60
	·11159	57·14	42·7	−·669	−4·91	60
	·11229	57·31	42·7	−·669	−4·89	30
	·11280	57·38	42·9	−·670	−4·88	30
	10·12162	20 09 10·70	−45 39 30·0	−·686	−4·35	120
	·12283	10·81	29·9	−·687	−4·31	60
	·12352	10·91	29·5	−·687	−4·29	30
	22·13422	20 32 40·94	−44 34 59·5	−·684	−3·46	600
	·13880	41·38	58·1	−·684	−3·31	135
1941 Mar.	1·12498	20 43 43·90	−43 54 21·1	−·676	−3·43	600
	7·12591	20 51 48·21	−43 23 36·7	−·668	−3·09	600
	·13613	48·97	34·0	−·662	−2·76	900
1941 Apr.	1·14858	21 12 46·44	−42 22 26·1	−·554	−0·94	1205
	·16104	46·76	27·8	−·524	−0·62	905

Van Gent's Comet

Date	U.T.	R.A. (1941·0)	Dec.	Parallax × Distance		Exposure
	d	h m s	° ′ ″	s	″	s
1941 June	11·77451	16 36 37·44	−26 49 38·4	−·434	−2·34	600
	·78005	35·22	49 09·4	−·419	−2·25	180
	16·84850	16 02 54·22	−19 06 57·8	−·108	−2·28	180
	·85161	52·80	06 38·0	−·098	−2·27	120
	30·82063	14 40 49·39	+ 4 33 29·9	+·103	−5·44	300
	·82450	48·10	33 47·6	+·115	−5·44	180
	·82726	47·18	+ 4 34 06·9	+·123	−5·43	180

Notes on the Plates made by the Measurer

De Kock's Comet.—Images poor and nucleus indefinite on January 21, 27, February 25, 27. On January 24 the nucleus appeared double. The brighter south component was measured. Separation about 0·2 mm. = 12″.

Cunningham's Comet.—For the plates taken on the first two mornings the stronger images were best. On February 22 images were faint and diffuse.

Van Gent's Comet.—Images very faint and trailed. Hardly visible, especially on June 30.

SOME NOTES ON COMET 1941*c* (DE KOCK)

R. H. Stoy, M.A., Ph.D.

(Communicated by H.M. Astronomer)

This comet was accidentally discovered on the morning of 1941 January 15 by Mr. R. P. de Kock of Pearl, Cape Province, South Africa. Mr. de Kock, who is a keen variable star observer, was setting his telescope on R Lupi when he first noticed it. The head showed clearly, while the tail was well developed and at least half a degree long. Its estimated magnitude was 5·8. Mr. de Kock immediately reported his find to the Cape Observatory which, in turn, telegraphed the information to the Union Observatory at Johannesburg where the first photographs of this comet were obtained.

At the time of discovery the comet was an easy object for binoculars in the morning sky. It was still approaching the Sun and the Earth, so that its brightness and motions southwards and eastwards were rapidly increasing. By the time it had overtaken the Sun in right ascension, it had moved so far south that it had become for the Cape a circumpolar object, though it was never very high in the sky during the night. As a naked-eye spectacle, the comet was probably at its best on the evening of Sunday, February 2, when the head was of the second magnitude and the tail at least five degrees long. From that time on its light was swamped by that of the waxing Moon, and by the time that the Moon had left the evening sky the comet had grown relatively faint and inconspicuous.

The comet was photographed with the Cape Astrographic Refractor on eighteen days between January 20 and March 6, twenty-four plates in all being obtained. These photographs were primarily intended for use in measuring the position of the comet, but wherever possible exposures guided on the comet and long enough to register the structure of the head were obtained. The times at which these plates were taken together with the positions of the comet derived from them have already been given.* These notes are an attempt to describe the principal physical features of the comet as recorded on them.

These notes are based on an examination of the plates with a low-power eyepiece and on measurements of drawings made from them. The plates were projected on to a piece of paper with the help of a first-class enlarging lens and a 500-watt lantern, and the main features of the comet sketched in. At least three such drawings of each plate were made. The orientation of the drawing and position angles were derived from the lines joining stars whose positions were known. Usually three of the reference stars used in deriving the position of the comet were selected for this purpose. A magnification of 8·7 diameters was used throughout.

After the drawings and measurements had been completed, an attempt was made to match the outlines of the observed caps by known curves. Series of parabolas and catenaries of different sizes were therefore plotted on graph paper, cut out and placed in turn over the drawings. In nearly every case it was possible to find a catenary that fitted satisfactorily. The parameter (c) of this catenary was therefore included in the dimensions of each cap. The other dimensions given are the distance of the vertex from the nucleus and the width of the cap at the nucleus.

The early appearance of Comet de Kock had much in common with that of Donati's Comet of 1858 which was so elaborately described and figured by G. P. Bond.† In

* See the previous paper.

† *H.A.*, 3, 1, 1862.

fact many of his illustrations (*e.g.* Plates 33, 34 and 36) might easily be taken as reproductions of drawings of Comet de Kock.

The dark division between the two principal tail streamers that is so noticeable a feature of these drawings was very conspicuous in Comet de Kock. As the comet approached the Sun and the Earth (perihelion was at January 27·8 and the closest approach to the Earth was a few days later) this dark cleft appeared to become broader and more diffuse, and on February 2 it seemed to be completely absent. On that day it was almost as though the two streamers had overlapped and the tail was relatively narrow and brightest along its centre. By February 4 the cleft had reappeared and thereafter seems to have got steadily narrower and more pronounced.

The envelopes (or caps) were very similar in both comets. As far as can be seen from the present series of plates, the caps were of fairly uniform brightness except near their rear tips which were brightest at the edges. In the case of one or two of the inner caps, the distribution of luminous matter was far from uniform, the brightest portions being just inside the rim proper. The shapes of most of the caps could be very satisfactorily represented by catenaries. The few cases where they could not have been noted, and except for February 2, are chiefly inner caps. In all these cases the departure from a catenary was in the sense that the observed curve was less divergent near its open end than was the catenary that fitted it best near its vertex, the catenary, in its turn, being, of course, less divergent than the corresponding parabola.

On the fountain theory of the formation of these caps as outlined by Eddington in his beautiful discussion of the envelopes of Comet Morehouse * such a departure would indicate that the velocity of outflow from the nucleus of the matter forming these envelopes was steadily increasing. If this were so, one would expect the linear size of the caps to increase from day to day. Though the data from these plates are not conclusive, they seem to indicate that, from January 20 to 28, the exact opposite was the case for the inner envelopes. The caps grew brighter as they got smaller, and on the days they disappeared the nucleus was obscured by bright nebulosity. For the outer caps there is not the same amount of evidence available. What there is seems to show that these outer caps remained much about the same size, or in some cases even expanded slightly before they started to contract. In passing, it may be noted that the nucleus is very approximately at the centre of curvature at the vertex of the representing catenary, not at half this distance as it would be if it were near the focus of the best fitting parabola.

In the notes that follow an attempt has been made to describe the phenomena visible on the plates as accurately and as free as possible from preconceived ideas of what ought to be there, in the hope that, in combination with similar observations, they may be of some use in helping to discover the mechanisms that were at work in the shaping of this comet. The numbers in the brackets that follow the date at the head of each note are (1) the P.A. of the line joining the comet to the Sun, (2) the P.A. of the comet's motion, (3) Δ, the distance of the comet from the Earth in astronomical units, and (4) the corresponding linear equivalent in kms. of 1″.

Measurements of the details of a comet are notoriously difficult; this was especially true of these plates which are not on a very large scale (1 mm. $\equiv$ 1′) and on which the low degree of contrast rendered very hard the task of determining the boundary lines between parts that did not differ greatly in brightness. (The plates were Ilford Zenith 700 developed in Amidol; the resulting softness had the advantage of enabling features of the comet which differed very greatly in brightness to be registered simultaneously.) In view of their uncertainty most of the measurements given have been rounded off to the nearest 5″. In the case of the dimensions given for each cap, the parameter of the representing catenary was found quite independently of the measurements at the nucleus

* *M.N.*, 70, 442, 1910.

and in general will not be quite congruent with them. For the smaller caps, the greatest error probably lies in the value given for c, but for the larger ones the least reliable measurement is that of the distance of the vertex from the nucleus.

1941 *January* 20. (87°·9; 137°; $\Delta = 0{\cdot}507$; 365 kms.)

The shortest exposures (5 and 15 seconds) show only a sharply defined nucleus and faint traces of two fan-like emissions from it, the longer and brighter in P.A. 30°, the other in P.A. 150°. In the 1-minute exposure these emissions are merged to form a well-defined cap with clear-cut edges, roughly semicircular in shape and about 35″ in radius. The northern edge, which is the brightest part of the cap, is very slightly extended beyond the bounding diameter which is in P.A. 0°.

The 15-minute exposure shows that this cap is superimposed on a larger fainter one which seems to be continuous with the tail of the comet. The dimensions of this cap, which can be well represented by a catenary with $c = 50''$, are $65'' \times 145''$. Its axis of symmetry is in P.A. 269°. A faint circular coma entirely surrounding the head is also faintly recorded. On the 27-minute exposure this coma is clearly visible. It appears to be circular and to extend uniformly in all directions to a distance of about 150″.

These exposures do not record the fainter details of the tail very well. They give the impression, however, that the tail consists of a very faint background on which are superimposed two bright streamers diverging from the head of the comet and apparently associated with the bright inner envelope. The southern streamer is the stronger. Its northern edge is fairly clear cut and lies along the direction joining the Sun to the comet, *i.e.* in P.A. 268°. Its southern boundary, which is not so sharp, is in P.A. 265°. The northern streamer is spread out over the eight degrees between P.As. 273° and 281°. Between these two streamers there appears a well-defined dark space which would stretch right up to the nucleus were it not for the spherical coma that surrounds the whole head.

1941 *January* 21. (85°·3; 134°; $\Delta = 0{\cdot}470$; 340 kms.)

The 30- and 60-second exposures show that the inner semicircular cap has become much brighter relatively to the nucleus, which is not so clearly differentiated from it as it was on the previous day. There are still signs of the two nuclear emissions. The short stubby one in P.A. 150° is not greatly altered, but the one whose centre line was in P.A. 30° is stronger, narrower and more sickle shaped in form. The handle of this sickle is in P.A. 5° and accentuates that part of the straight bounding edge of the cap, while the blade is parallel to, and lies just inside the north-eastern portion of the curved edge. This emission makes the northern part of the cap much brighter than the southern part. The radius of this cap is about 30″.

The longest exposure (which was only 5 minutes) indicates that the brightest features of the head and tail have not altered greatly. The tail streamers seem to be associated with the cap that immediately surrounds the bright semicircular cap and which is just bright enough to register faintly on the 1-minute exposure. This cap extends for over 1′ behind the nucleus and does not appear to have a well-defined following edge. It can be satisfactorily represented by a catenary with $c = 55''$. The dimensions through the nucleus are $60'' \times 130''$ and its axis of symmetry is in P.A. 268°.

1941 *January* 22. (81°·8; 132°; $\Delta = 0{\cdot}435$; 315 kms.)

The nucleus is very bright and conspicuous. It consists of a condensation about 15″ in diameter surrounded eccentrically by a fainter elliptical envelope $20'' \times 30''$ with major axis in P.A. 130°. The nuclear emissions and the semicircular cap seem to have disappeared. The innermost cap that now appears is relatively much fainter and can be well represented by a catenary with $c = 35''$. Its dimensions are $50'' \times 120''$. The back edge of this cap lies some 20″ to the tailward side of the nucleus, but it is diffused and indefinite. The northern curved edge extends backwards into the tail to some 110″ from the vertex. There is a similar, but not so marked, cusp-like extension of the

southern edge, or rather of the whole of the southern half of the bounding chord. This extension is brightest at its two edges and merges with the southern tail streamer which on the 6-minute exposure, the longest available for this morning, seems to be broader and stronger than the northern one. The P.A. of the sharp inner edge of the southern streamer is 258°.

This inner cap is surrounded by another fainter one whose dimensions are approximately 80″ × 200″ and whose shape is that of a catenary with $c = 85''$. Its edges are not very distinct as it seems to be merged with a still fainter outer cap, not very much larger than it and almost coinciding with it except along the north-east edge. The axis of symmetry of the two inner caps is in P.A. 257°.

1941 *January* 23. (76°·5; 129°; $\Delta = 0.400$; 290 kms.)

The nucleus is relatively bright and almost stellar. The inner cap is very similar in shape to that of the previous day, but it does not stretch so far back into the tail and its brightness is more concentrated towards the curved edge, especially in the northern part. The dimensions of this cap are 45″ × 100″, while the parameter of the catenary that best represents it is 33″. The tips of the curved edges extend to about 75″ from the vertex.

The 30-minute exposure records faintly about 50′ of the tail. This does not differ greatly in general appearance from that on January 20. The dark cleft between the two principal streamers of the tail is broader and not so clearly marked. The P.As. of its edges are about 260° and 265°. The brightness of the northern streamer between its two edges is fairly uniform. The southern streamer, however, is brightest along its inner edge, which is very sharply defined, and gradually fades to the southern (outer) edge, which is hazy and ill defined. The southern streamer is now slightly the broader of the two.

The outlines of two caps which surround the inmost one and which stretch away back into the tail can be made out. Their dimensions are 75″ × 200″, $c = 65''$, and 125″ × 320″, $c = 110''$, while their axis of symmetry is in P.A. 258°. The tips of the curved edges of the first of these two caps are 260″ behind the vertex on the south side and 220″ on the north side. The second of these two caps seems to be continuous with the outline of the faint background of the tail, but the axis of symmetry of this outline at some distance back from the head seems to be in P.A. 263°.

The circular coma that uniformly surrounds the head is recorded to a distance of about 3′·5 from the nucleus. It seems to fade out gradually towards its edges.

1941 *January* 24. (70°·9; 124°; $\Delta = 0.368$; 265 kms.)

The longest exposure obtained on this morning was 30 seconds, so that only the brightest features of the inner cap are recorded. This cap is reminiscent of that on January 21. It is roughly semicircular in shape with the nucleus indistinct and slightly elongated in P.A. 120° lying on the bounding diameter. A sickle-like emission from the nucleus brightens the north-west edges of the cap, which is about 35″ in radius.

A larger cap surrounding this one is also very faintly recorded. Its dimensions seem to be about 75″ × 160″, $c = 65''$. The axis of symmetry is in P.A. 245°.

1941 *January* 25. (62°·0; 120°; $\Delta = 0.338$; 245 kms.)

For this morning there is a 45-minute exposure available, but unfortunately, owing to the sighting of Cunningham's Comet, nothing between that and a 15-second one, so that details of the inner part of the head are missing.

The nucleus is bright, distinct and almost stellar. Its photographic magnitude, judging from that of a nearby star C.P.D. 51° 10535, must be about seven. To the naked eye the head of the comet looked about as bright as α Arae, whose visual magnitude is 2·97.

Though the 15-second exposure shows traces of a larger fainter cap, it records nothing resembling the bright semicircular cap seen on the previous day. On the 45-minute exposure the head is naturally heavily over-exposed and the inner caps can only be made out with difficulty. The dimensions of the innermost one, in which the bright matter is slightly concentrated towards the edges, are about $80'' \times 180''$, $c = 65''$, though this catenary does not represent the open end of the cap too well, being too divergent. The cusps, *i.e.* the ends of the curved edges, of this cap are about $140''$ behind its vertex. The cap just outside this one is about $110'' \times 260''$, $c = 90''$ and ends about $330''$ behind its vertex. In this case too the catenary is slightly too divergent near the open end, but not so markedly as for the inner cap. The axes of symmetry of these two caps pass through the nucleus and lie in P.A. 243°. The cap bounding the head of the comet has dimensions of the order of $160'' \times 390''$, $c = 140''$, while its axis of symmetry is in P.A. 247°. It must be remembered, however, that it is impossible to trace the vertex of this cap with any certainty as it merges with the uniform coma that surrounds the head and which is registered on the 45-minute exposure to a distance of 10′ from the nucleus.

The general background of the tail is fairly uniform in structure, but is perhaps a little brighter towards the edges, especially near the head of the comet. 20′ back from the nucleus it is about 16′ wide and at 40′ back about 26′ wide.

Superimposed on this general background is the brightest feature of the comet's tail, a narrow straight streamer. Its northern edge, which is remarkably straight and clear cut, is in P.A. 245°. For the first 20′ from the nucleus the southern edge of this streamer is nearly as sharp as the northern one to which it appears parallel, but beyond that limit it becomes more diffuse and merges into the general background. The width of the parallel part near the nucleus is about 1′.

The dark marking in the tail is visible, but it is wider than it was and more diffuse, especially on the north side. It is not completely black and in fact probably only appears dark in contrast to the bright streamer that forms its southern edge.

1941 *January* 26. (49°·9; 112°; $\Delta = 0{\cdot}313$; 225 kms.)

In addition to the nucleus, which is bright, small but perhaps not quite stellar, the 5-second exposures show an elongated patch of nebulosity about $15'' \times 60''$. The 90-second exposure shows that this nebulosity is really the northern and brightest portion of the inmost cap whose dimensions are $60'' \times 130''$, $c = 50''$ and whose axis of symmetry lies in about P.A. 240°. The catenary fails to represent the form of the cap near its tips, which are about $80''$ behind the vertex and which, relatively to the catenary, are bent in towards the axis. The southern portion of the cap is fainter than the rest and is slightly diffuse. There is a cusp-like deformation of the bounding chord near its middle point due to a nuclear emission in P.A. 230° which is presumably the source of the long narrow streamer that is so prominent a feature of the tail.

Another cap surrounding this one is faintly recorded on the 90-second exposure. Its dimensions are about $100'' \times 230''$, $c = 90''$, and it extends to about $270''$ behind its vertex. On the 30-minute exposure this cap is seen to be surrounded by still another one whose dimensions are about $130'' \times 310''$, $c = 120''$. The P.A. of the axis of symmetry of these two caps is about 231°.

The strongest features of the tail can be traced out to about 1° from the nucleus. They are much the same as on the previous day. The narrow straight streamer is in P.A. 235° and can be traced out to nearly a degree from the nucleus. The dimensions of the cap that limits the background of the tail are about $180'' \times 420''$, $c = 170''$, while the P.A. of the axis of symmetry of this background up to about 15′ from the nucleus is about 237°. Its width at this point is about 15′. Beyond it the southern edge of the tail seems to bend round parallel to the long narrow streamer, while the northern edge seems to become roughly rectilinear and makes an angle of about 15° with the streamer.

As a consequence at about 50′ from the nucleus the southern edge of the tail lies only about 7′ south of the streamer, but the northern edge is about 17′ north of it.

There are still signs of the relatively dark cleft in the tail, but it is no longer bounded on the south by the streamer, nor does it stretch right into the nucleus. Its edges, which are in P.As. 245° and 250°, are vague and diffuse, while the space between them is by no means completely dark.

The dimensions of the uniform coma at the head of the comet as recorded on this 30-minute exposure are 8′ along the axis of the comet and 7′ perpendicular to this direction.

1941 *January* 27. (33°·6; 101°; $\Delta = 0{\cdot}292$; 210 kms.)

The shortest exposures show a small but rather diffuse nucleus with a very strong emission in P.A. 330°. This emission is nearly as bright as the nucleus itself. On the 15-second exposure it is about 25″ long and shows signs of fanning out towards the Sun. The 1-minute exposure shows it as a sickle-like formation reminiscent of those present on January 21 and 24, but perhaps in this case a comma would form a better simile as the curved portion is so much the fainter part of the emission. The whole of the inner cap with which it is associated can be traced out on the 5-minute exposure. It is roughly semicircular in shape, the straight edge being in P.A. 315° and the radius about 50″. The brightness of this cap decreases from the emission already described to the southern edge of the semicircle, which is diffuse and not very clearly defined. The small streamer in P.A. 220° is also recorded, but it is not nearly so strong as the brightest parts of this cap.

Two other caps surrounding this one are also recorded. The dimensions of the inner one, which extends to about 200″ behind its vertex, are $100'' \times 220''$, $c = 85''$, and of the other one about $140'' \times 350''$, $c = 120''$. The brightest part of the inner one is its northern edge. Its axis of symmetry is in P.A. 225°.

Little of the tail proper is recorded on this 5-minute exposure, but the long narrow streamer can be traced out for some distance. It is in P.A. 220°.

1941 *January* 28. (12°·3; 89°; $\Delta = 0{\cdot}277$; 200 kms.)

There is no trace of the bright inner envelope observed on January 27. The nucleus is small, bright but not stellar. It merges with a small circular patch of nebulosity which is brightest at the centre and fades out towards the edges. On the 5-second exposure this nebulosity is about 15″ in diameter, on the 15-second one about 25″ in diameter, and on the 3-minute one about 40″, though no great reliance can be placed on these figures as the object was low in the sky and the seeing far from good.

One cap is recorded on the 3-minute exposure. Its dimensions are $70'' \times 200''$, $c = 70''$, and it extends to 140″ behind its vertex, while the P.A. of its centre line is about 200°. The north-western edge and cusp, which is the greatest part, is clearly defined, but the eastern edge is rather diffuse.

1941 *February* 2. (276°·2; 38°; $\Delta = 0{\cdot}322$; 235 kms.)

Even in the shortest exposures (5 seconds) the nucleus proper is all but hidden by a very bright elliptical shell that surrounds it. The nucleus is rather to one end of this shell which stretches out from it in P.A. 295°. Its dimensions are about $30'' \times 20''$. On the 30-second exposure this shell is beginning to be merged with a general fan-like emission from the nucleus. This emission, which is nearly 50″ long, has fairly sharp edges in P.As. 215° and 310°. Its brightest part is along the direction of the axis of the nuclear ellipse.

The 1- and 2-minute exposures show the cap with which this emission is associated and also an outer one surrounding it, but unfortunately they overlap each other as the telescope was not moved sufficiently between the two exposures. In any case they are

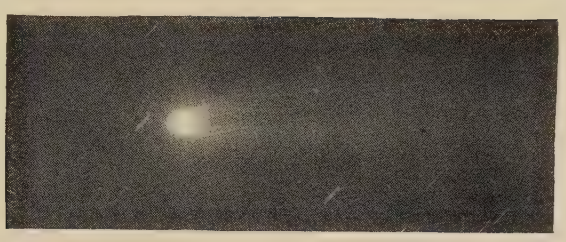

1941 January 20.

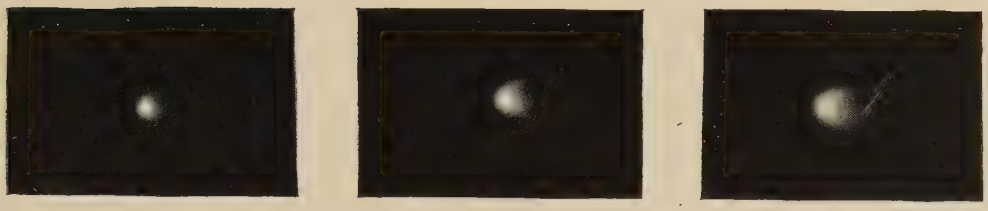

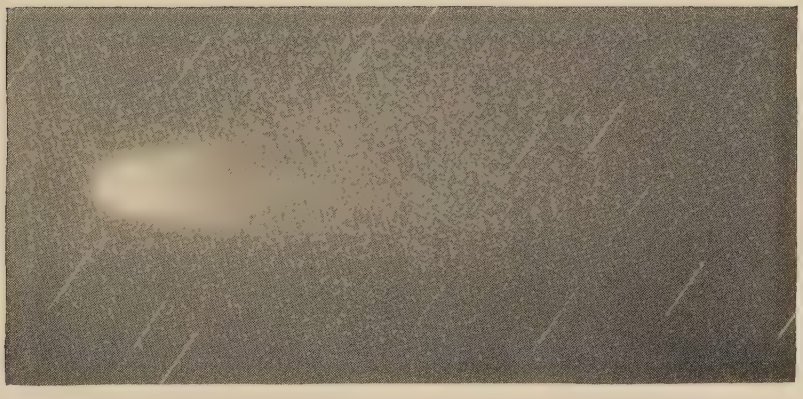

1941 January 26.

1941 February 2.

rather too blurred by the motion of the comet during the time of exposure to be of much use. The only other exposure available is a 45-minute one, and on this the bright portions of the head are of course very much over-exposed so that the bright inner cap and two others surrounding it can only be made out with more than ordinary difficulty.

The inner cap is too small to say what form its curved edge really has or whether it has an axis of symmetry. What is noticeable about it is that it subtends an angle of less than 180° at the nucleus. Very approximately the curved edge can be represented by a catenary with $c=30''$ and with axis in P.A. 76°. The straight edges are in P.As. 175° and 320° and are about 30″ and 50″ long respectively.

The two caps surrounding it have their axes in P.A. 100° and dimensions about $80''\times 210''$, $c=75''$, and $125''\times 300''$, $c=100''$, but a catenary is not a really satisfactory representation of any of the caps visible on this day. The caps actually observed are all less open curves. On the southern side these caps end in fairly well-defined cusps about 180″ and 400″ behind their respective vertices, but on the northern side their ends are not so clearly marked, and though the caps proper do not extend so far from the nucleus as on the south side, yet the continuation of their curved edges can be followed out for a great distance into the tail.

Though the tail is recorded faintly to over one and a half degrees from the nucleus it is not recorded sufficiently strongly to render the faint and elusive detail at all clearly. The dimensions of the cap that bounds the faint even background of the tail are about $190''\times 400''$, $c=130''$. The breadth of this background about 1° back from the head is 18′. Superimposed on it are a number of streamers, the brightest of which lies between P.As. 103° and 108°. About 10′ from the nucleus a rather narrow streamer branches off from this one in a direction whose P.A. is 99°.

There is no sign of a circular halo round the head on this plate nor of a dark space in the centre of the tail, in fact the centre is the brightest portion of the tail.

1941 *February* 4. (266°·5; 35°; $\Delta=0.379$; 275 kms.)

The shortest exposures (5 seconds) show a bright clear-cut stellar nucleus with traces of a fan-like emission, the straight edges of which are in P.As. 190° and 330°. On the 5-minute exposure—the longest available for this day—this emission is seen to be the brightest parts of a cap which is roughly like the sector of a circle in shape. The radius is about 50″. The straight edges, which are in P.As. 190° and 330°, are not sharp as the cap appears here to shade off rapidly into two broad streamers which are superimposed on the faint background of the tail.

This bright inner cap is surrounded by a much fainter one, the dimensions of which are $80''\times 180''$, $c=70''$, and whose axis of symmetry is in P.A. 88°.

From the small part recorded (only about 5′, and that faintly) the tail appears to be similar to that on January 20 rather than to that on February 2. The southern of the two streamers mentioned above is the broader and brighter. Its northern edge in P.A. 93° is especially sharp and bright. Between this edge and the southern edge of the northern streamer which is in P.A. 84° is a narrow dark space which seems to extend right from the nucleus outwards.

A halo round the whole head is faintly recorded up to about 2′ from the nucleus.

1941 *February* 7. (260°·1; 33°; $\Delta=0.482$; 350 kms.)

The general appearance of the comet is very similar to that on February 4, though the 5-minute exposure does not record nearly so much of the comet as it did. The bright inner cap has a radius of 35″, while its straight edges are in P.As. 180° and 320°. The emissions that form this cap are noticeably strong between P.As. 180° and 190°. The dimensions of the faint outer cap are $70''\times 150''$, $c=50''$, while its axis is in P.A. 84°. The inner edges of the two broad streamers that enclose the dark space in the tail leave the nucleus in directions whose P.As. are 90° and 72°.

1941 *February* 9. (258°·1; 32°; $\Delta = 0{\cdot}557$; 400 kms.)

The 10-second exposure records a bright but not quite stellar nucleus, the 1-minute exposure records the bright inner cap, while the 10-minute exposure records a fainter cap outside this one and also about 20′ of the brighter features of the tail.

The bright inner cap is similar to that seen on February 4 and 7, except that the straight radial edges have, as it were, moved parallel to themselves about 25″ backwards into the tail streamers, while the transition of cap to tail streamer is very much more gradual. The light in these streamers is now more concentrated to the inner edges (which lie in P.As. 79° and 83°) so that the dark gap between them is even more pronounced. The southern streamer is still the stronger of the two.

The dimensions of the two caps are 40″ × 85″, $c = 30''$, and 70″ × 170″, $c = 55''$. The axis of symmetry is in P.A. 77°.

The Royal Observatory,
Cape of Good Hope:
1941 *July.*

THE CASSEGRAIN TELESCOPE AS A THICK LENS

H. C. Plummer, F.R.S.

(Received 1941 September 4)

1. Since the reflecting telescope has two reflecting surfaces a great variety of forms might be expected, especially as modern technique has brought any desired figure within the bounds of possible attainment. In reality the practical choice is by no means so wide. The possibility of using the main mirror alone at its focal plane is too important to be readily sacrificed for the sake of an advantage to be gained by use in combination. Hence it must receive a parabolic figure. The axial rays being thus brought to a point, the aplanatic condition * imposes the figure of a secondary mirror, defined by $r \pm r' = \text{const.}$ When the position of the focus is chosen, this means one of a family of confocal surfaces, elliptic (Gregory) or hyperbolic (Cassegrain). In the first case the two mirrors produce aberrations of like sign; in the second the aberrations are of opposite sign and compensation is possible. For this reason the Cassegrain form has been adopted, and it does not seem likely that the larger instruments will depart from it. The liberty of choice in the design is considerable, but it is not unlimited. Different purposes can of course be met by supplying more than one secondary mirror for use in one instrument.

2. The elementary (Gaussian) geometrical optics of the Cassegrain telescope depends on three elements, the curvatures of the two surfaces and their separation. Now these are precisely the characteristics of a single thick lens. The analogy is complete, and the theory of the lens can be adapted to the telescope directly. The first and third media are air. In the telescope the intervening medium is also air, but the two reflexions in the place of refractions require the refractive index to be treated as $\mu = -1$ in the usual way. The difference is not one of principle, but only of scale. Even in the refractor the thickness of the object-glass has sometimes been treated too lightly. Thus the focal length of the Lick 36 in. was once reported as 674 in., and this figure can probably still be found. But this is merely the length of the tube; the actual focal length, as determined from star measurements, is nearer 694 in.

Though the elementary theory of the Cassegrain telescope can be derived immediately from the theory of the thick lens given in any suitable text-book, it may yet be interesting to obtain it directly from first principles for the particular combination in view.

3. Let the axis meet the mirrors in the points A, B separated by the distance $AB = c$. Let O_1, O_2 be the centres of curvature of the mirrors, the radii being $AO_1 = a$, $BO_2 = b$. Thus $O_2O_1 = a - b - c$.

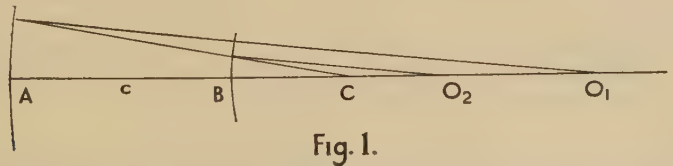

Fig. 1.

The line joining the ends of parallel radii meets the axis in the centre C of the combination, so that

$$\frac{CO_1}{CO_2} = \frac{a}{b}, \qquad \frac{CO_1}{O_2O_1} = \frac{a}{a-b}, \qquad \frac{CO_2}{O_1O_2} = \frac{b}{a-b}$$

or

$$AC = a - a\left(1 - \frac{c}{a-b}\right) = \frac{ac}{a-b}, \qquad BC = b - b\left(1 - \frac{c}{a-b}\right) = \frac{bc}{a-b}.$$

* The idea of this condition goes back to Descartes (*Dioptrique*, 1637).

If N is the conjugate focus of C for the mirror B,

$$\frac{1}{BN}=\frac{2}{b}-\frac{1}{BC}=\frac{2c-a+b}{bc}, \qquad BN=\frac{bc}{2c-a+b},$$

and if n is the conjugate focus of C for the mirror A,

$$\frac{1}{An}=\frac{2}{a}-\frac{1}{AC}=\frac{2c-a+b}{ac}, \qquad An=\frac{ac}{2c-a+b}.$$

The positions of the nodal points N, n are thus determined.

But for any ray reflected at both surfaces, and meeting the axis at distances u, u' in front of A and v', v behind B,

$$u'=v'+c, \qquad \frac{1}{u'}=\frac{2}{a}-\frac{1}{u}, \qquad \frac{1}{v'}=\frac{2}{b}-\frac{1}{v},$$

so that

$$\frac{au}{2u-a}-\frac{bv}{2v-b}=c,$$

$$2uv(2c-a+b)-bu(2c-a)-av(2c+b)+abc=0,$$

$$\left\{u-\frac{a(2c+b)}{2(2c-a+b)}\right\}\left\{v-\frac{b(2c-a)}{2(2c-a+b)}\right\}+\frac{a^2b^2}{4(2c-a+b)^2}=0.$$

Hence

$$\left\{u-An-\frac{ab}{2(2c-a+b)}\right\}\left\{v-BN+\frac{ab}{2(2c-a+b)}\right\}+\frac{a^2b^2}{4(2c-a+b)^2}=0$$

or

$$\frac{1}{u-An}-\frac{1}{v\ \ -N}=\frac{2(2c-a+b)}{ab}=\frac{1}{f}.$$

Now for rays incident on the first mirror $u=\infty$, and thus the position of the focus F is given by

$$BF=v=BN-\frac{ab}{2(2c-a+b)}=\frac{b(2c-a)}{2(2c-a+b)}.$$

The focal length f and the positions of the focus F and the corresponding nodal point N are all that are required.

Here of course a difference between the telescope and a thick lens appears. The lens and the object can be reversed relatively to one another. For the telescope this has only a theoretical, not a practical meaning, since it is not feasible to reverse the order of incidence on the two mirrors. In this theoretical sense $v=\infty$, there is another nodal point n, the focal length f is unchanged, and the other focus F' is given by

$$AF'=An+f=\frac{a(2c+b)}{2(2c-a+b)}.$$

4. For the first example the Victoria telescope may be taken. Here

$$a=722{\cdot}8 \text{ in.}, \qquad b=238{\cdot}5 \text{ in.}, \qquad c=275{\cdot}2 \text{ in.},$$

and for the centre C of the combination

$$AC=\frac{ac}{a-b}=410{\cdot}7, \qquad BC=\frac{bc}{a-b}=135{\cdot}5.$$

Since $2c-a+b=66{\cdot}1$, the nodal points are given by

$$BN=\frac{bc}{2c-a+b}=993{\cdot}0, \qquad An=\frac{ac}{2c-a+b}=3009{\cdot}3,$$

while the focal length is

$$f=FN=F'n=\frac{ab}{2(2c-a+b)}=1304{\cdot}0.$$

If all distances are reckoned in front of the principal mirror, since $AN=1268{\cdot}2$,

$$\begin{array}{llll} AF=-35{\cdot}8, & AB=275{\cdot}2, & \tfrac{1}{2}AO_1=361{\cdot}4, & \tfrac{1}{2}AO_2=394{\cdot}45 \\ AC=410{\cdot}7, & AN=1268{\cdot}2, & An=3009{\cdot}3, & AF'=4313{\cdot}3 \end{array}$$

the unit being one inch.

5. As a second example, the figures *

$$a=9{\cdot}760 \text{ m.}, \qquad b=18{\cdot}408 \text{ m.}, \qquad c=2{\cdot}684 \text{ m.}$$

will be taken, so that $2c-a+b=14{\cdot}016$. For the centre C,

$$AC=\frac{ac}{a-b}=-3{\cdot}029, \qquad BC=\frac{bc}{a-b}=-5{\cdot}713$$

for the nodal points,

$$BN=\frac{bc}{2c-a+b}=3{\cdot}525, \qquad An=\frac{ac}{2c-a+b}=1{\cdot}869$$

and the focal length is

$$f=\frac{ab}{2(2c-a+b)}=6{\cdot}409.$$

Hence

$$\begin{array}{llll} AF=-0{\cdot}200, & AB=2{\cdot}684, & \tfrac{1}{2}AO_1=4{\cdot}880, & \tfrac{1}{2}AO_2=11{\cdot}888 \\ AC=-3{\cdot}029, & AN=6{\cdot}209, & An=1{\cdot}869, & AF'=8{\cdot}278 \end{array}$$

the unit being the metre.

6. The distribution of these points is also roughly indicated in fig. 2. Here A is the principal mirror, B the secondary, F is the focal plane and N the corresponding nodal

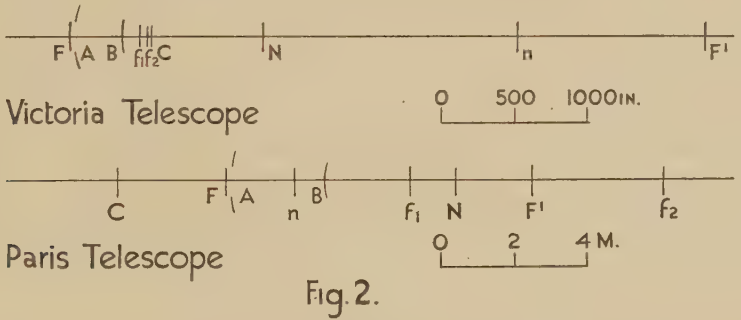

Fig. 2.

plane. The foci of the two mirrors are respectively f_1 and f_2. The centre of the combination is C, and F' and n are the corresponding focal and nodal planes when the order of incidence on the mirrors is reversed; these have only a theoretical significance.

The complete contrast between the two instruments seems very striking. This arises from the fact that in the Victoria telescope the focal length of the secondary mirror

* From Danjon et Couder, *Lunettes et Télescopes*, p. 196.

is comparatively short, while in the telescope designed for Paris the focal length is relatively very long. It is quite clear that the Cassegrain telescope is very far from having arrived at anything like a standard type.

7. In the older text-books the description of the Cassegrain telescope treats the eyepiece as an integral part of the instrument. In the modern use an eyepiece is a relatively unimportant accessory which may never be employed at all. For any purpose it is the position of the focal plane and the focal length which are of the first interest, and the latter is most simply determined by the corresponding nodal point, in this case identical with a principal point. But by the characteristic property of the nodal points any ray incident through n is finally reflected through N parallel to its original direction, and this is secured by the construction by which it is clear that the part of the ray between the mirrors passes through the centre C (fig. 1). The nodal point N is thus the position of an equivalent thin lens which represents the effect of the telescope.

The text-book has been wont to treat the telescope as a visual instrument, as the etymology of the word requires. The word now has a wider meaning; and apart from this the conventional treatment of the complete visual instrument was not free from an artificial element. For the text-book eyepiece demanded a text-book eye, focused on infinity. Now this does not represent the actual eye of the average observer; and since the function of the eyepiece is the same for all types of telescope, some advantage would be gained by discussing this function relative to the individual eye but apart from the nature of the image-forming instrument. The inclusion of the conventional eyepiece in the optical instrument has also a slight theoretical inconvenience in that the whole combination constitutes a *telescopic* system, which requires special consideration inasmuch as its nodal points are at infinity.

NOTE ON THE ORIGIN OF PLANETS AND SATELLITES

R. A. Lyttleton

(Received 1941 September 9)

The demonstration that a rotating mass of gravitating liquid becomes ordinarily unstable at the last Jacobian figure rests on the usual simplifying assumptions of problems of oscillations of dynamical systems—that is, all displacements and velocities are regarded as small and second-order terms are neglected. The subsequent finite motion raises theoretical difficulties of so complex a nature as to make it impracticable to attempt to discover directly the ultimate outcome of the instability. The question may nevertheless be capable of being definitely settled, for the system must move to some other stable state of steady motion and if the number of essentially different stable states is limited then clearly it might prove possible to decide between these on the basis of general considerations without actually solving in detail the intermediate motion. It appears that the present problem can be discussed successfully in this way.

To begin with, it is evident that the mass must become disrupted, for there is no stable configuration for it to occupy as a single body. Furthermore, since the instability affects the mass as a whole and does not take the form of neutral points occurring on the free surface, the conclusion that the mass breaks into a number of pieces of comparable sizes would seem to be unavoidable and it has been accepted in agreement with previous writers that there would be two main components. It is then found that the requirement that whatever motion takes place shall be capable of complete reversibility eliminates the possibility of the system coming to a steady state of finite relative motion of the two parts and consequently they must separate with hyperbolic velocity. The final steady state accordingly consists of two independent stable masses receding with constant velocity.

Always having due regard to the limitations of its derivation a result of this kind clearly represents a useful guide cosmogonically, for such investigations are concerned largely with the states in which systems are likely to remain for long periods rather than with exact details of the motion by which successive states are connected. Having decided the general nature of the final state it is then possible to estimate the mass-ratio of the two component masses by considerations of the energy and angular momentum of the critical ellipsoid. It can be shown quite definitely that a lower limit exists for the mass-ratio having a value very different from unity. This lower limit arises since the minimum internal energy for the components corresponds to their having zero rotation. The energy of the last stable ellipsoid is then to be compared with that of two spherical masses at infinite distance apart. This condition was investigated previously *, but a referee of a more recent paper † has called my attention to the fact that the value of the gravitational energy of this ellipsoid originally adopted is numerically incorrect. To the order of accuracy required, the proper value is

$$-0{\cdot}890GM^{5/3}\rho^{1/3}$$

and this represents a more exhausted state than that implied by the earlier calculations. The available energy consisting of the sum of the gravitational and rotational energies is therefore less than that given originally and the actual value is

$$-0{\cdot}745GM^{5/3}\rho^{1/3}.$$

* *M.N.*, 98, 646, 1938. † *M.N.*, 101, 216, 1941.

This correction alters the limit for the mass-ratio of the components; the mass-ratio $m/(1-m)$ must satisfy the revised condition

$$0{\cdot}745 < 0{\cdot}967\{m^{5/3}+(1-m)^{5/3}\}$$

or

$$m^{5/3}+(1-m)^{5/3} > 0{\cdot}77$$

and this requires $m < 0{\cdot}19$ about, giving a limiting mass-ratio of rather more than 4 : 1. In any real case the mass-ratio must exceed this value, for the components will inevitably possess a certain amount of rotation.

It is clear that this revised estimate of the mass-ratio will also affect the question of the conservation of angular momentum. Previously it was found that if the radial and transverse velocities of the two components at separation were equal the available angular momentum would lead to a mass-ratio of 3·6 : 1. Evidently for a larger mass-ratio than this the transverse velocity component would be larger, and it therefore appears that the initial transverse velocity of separation may itself closely approach the velocity required for escape. If the whole energy is carried in this transverse velocity the corresponding condition provided by the angular momentum is

$$1{\cdot}66 \geqslant m^{5/3}+(1-m)^{5/3}+6m(1-m)\sqrt{m^{1/3}+(1-m)^{1/3}}$$

and the limiting mass-ratio is a little greater than 7 : 1. Accordingly, since the rotations of the components will take some of the available energy it appears that the mass-ratio of the components into which the body divides must be at least 6 : 1 or even higher.

A point that may perhaps be emphasised in the present connection concerns the question of the angular velocity. It will be recalled that the discussion of the evolution of a rotating mass is facilitated if the fluid is regarded as remaining of constant density while the angular momentum slowly increases, the series of figures so occurring being completely equivalent to development with constant angular momentum accompanied by steadily increasing density, this latter situation being evidently of the kind more likely to occur in natural problems. In the first case of increasing angular momentum it is to be noticed that the angular velocity takes a maximum value at the point of bifurcation of the Jacobian series from the Maclaurin series, secular stability at the same time transferring to the former series. Thus the angular velocity begins at zero for the spherical form and increases all along the spheroidal series to this maximum and thereafter decreases along the ellipsoidal series. This feature of the development, which does not seem to have been generally recognised, may very well be of particular importance, for it shows that when the ellipsoid breaks up the component masses may take up spheroidal form practically at once without necessarily undergoing any considerable change in angular velocity. Thus slow rotation accompanied by stability may come to be imparted to the components by the same process that leads to the disruption of the original mass.

Formerly the limiting mass-ratio was estimated at about 3 : 1 and it was therefore suggested that Jupiter and Saturn may have originated from a single mass, but clearly this possibility cannot now be retained unless the initial mass-ratio has been reduced as a result of some increase of mass by these planets since this stage of their formation. However, a number of lines of evidence suggest that such an increase could actually have taken place. Thus in the first instance it may be remembered that the mechanism of the origin of the planetary material is such that the greater portion of the lightest gases would probably escape from the initial condensations though not necessarily from the field of the Sun. On this basis the primitive planets would consist largely of the heavier elements, the density of the main mass of such bodies when liquefied would be of order 3 or 4 gm. per c.c. at very least and for fission to occur would require a rotation period of the order of three hours at most. Hence the initial rotation speeds of the components are likely to have been of a higher order of magnitude than their present values and to

reduce them would require considerable addition of mass. Secondly, a source for such material is readily found in the resisting medium, itself formed by the lighter gases escaping at first. A mass of order 10^{30} gm. distributed uniformly through a volume of dimensions comparable with the radius of Saturn's orbit would have a density of order 10^{-14} gm. per c.c. and accretion by a planet having mass of order 10^{30} gm. moving at a few kilometres per second in such a cloud would be sufficient to double the mass of the planet in a period of about 10^7 years. The relative velocity of the planet and the medium would depend chiefly on the eccentricity of the initial orbit and the distance from the Sun, and therefore the more massive of two planets would not necessarily accrete more rapidly per unit mass. In this way on account of a lower relative velocity a planet like Saturn might increase in mass to a greater extent than Jupiter and thereby reduce the mass-ratio as compared with the original mass-ratio. Further, according to the investigations of Wildt and Jeffreys, these planets possess huge proportions of atmosphere-forming materials comparable in mass with that of the whole planet, and particularly is this so for Saturn. The mean density of the latter is only 0·7 while that of Jupiter is 1·3, and it is not possible to explain this by supposing that the atmosphere is of great depth and negligible mass. According to Jeffreys the mass of the outer part of Saturn comprised of the lightest materials is of order two-thirds the mass of the whole planet, while for Jupiter the corresponding fraction is about one-third, and these figures are confirmed by the more recent work of Wildt. If all this material is due to accretion of light gases the original mass-ratio may have greatly exceeded the present value.

The importance and necessity for the fissional mode of origin of the nuclei of the great planets arises of course in connection with the presence of satellite systems associated with every one of these planets. However, for this purpose it is not essential for Jupiter and Saturn to be regarded as having originated from a common primitive planet and it is seen at once that the possession of satellites and the origin of the terrestrial planets could be equally well explained if each of the four great planets had a separate fissional origin. The smaller components resulting from the fission could readily escape from the Sun in the same way as was previously suggested for the companion planets to Uranus and Neptune. Indeed there now appear to be several possible modes of origin of the four great planets; thus, all four may have had separate origins from four primitive planets and the other components escaped from the Sun, while secondly Jupiter may have had a common origin with Saturn or even Uranus or Neptune (the mass-ratio of these latter to Jupiter is about 1 : 16) and there are clearly other possible combinations involving a common origin for some planets and separate origins for others. Apart from the fact that it seems unlikely that Neptune and Uranus can have been formed from a single body, since their present masses and mean densities are so similar, it does not appear to be possible as yet to make any decisions between the remaining alternatives.

We have then the following general results. The evolution of a primitive rotating planet brings it to a state of ordinary instability that must bring about its division into a pair of masses eventually separating completely in hyperbolic motion. The mass-ratio of these components must be at least 6 : 1 and possibly higher. The manner in which the terrestrial planets and the satellite systems of the great planets may have formed is therefore the same as described in earlier papers, but there now appear to be several ways in which the various pairs of planets may be related. The simplest situation would be obtained by supposing that two primitive planets evolved by fission to produce Jupiter and Neptune say from one of them and Saturn and Uranus from the other; however, all four planets may have had separate origins and there are clearly possibilities intermediate between these two.

OBSERVATIONS OF OCCULTATIONS AT THE SOLAR PHYSICS OBSERVATORY, CAMBRIDGE, 1939–1940

(Received 1941 September 25)

The observations of occultations given in Table I below were made by stop-watch, compared with chronometer, by H. E. Butler and A. D. Thackeray. Corrections for personal equation of $-0^s.2$ to $-0^s.3$ were applied to the observed times in accordance with laboratory experiments on artificial occultations; in one case, the grazing occultation of 1940 November 10 *, a correction of $-0^s.5$ was applied. In the last column of Table I, letters in parentheses denote the instrument used, as follows:—

T Thorrowgood 8-inch refractor.†
N Northumberland 12-inch refractor.†
H Huggins 15-inch refractor.

These three telescopes are within a few yards of each other, and in the reductions of Table II, carried out by A. Ali, the standard position was used—

$$\rho \sin \phi' = 0.78664, \qquad \lambda = -0^m.375.$$

In the reductions the correction of $+1''.5$ to the Moon's longitude, appropriate to the years in question, was applied. The serial number is that in the *Nautical Almanac*, from which Occultation Reduction Elements were taken.

TABLE I

Serial No.	Star	Mag.	Phase	Date	U.T.	Observer (Instrument)
					h m s	
846	B.D. −15° 5626	6·2	D	1939 Oct. 20	17 45 33·5 **	H. E. B. (N); A. D. T. (T)
847	β Cap	3·2	D	Oct. 20	17 53 17·3 **	H. E. B. (N); A. D. T. (T)
847	β Cap	3·2	R	Oct. 20	19 04 26·2	A. D. T. (T)
890	B.D. +17° 750	6·2	R	1939 Oct. 30	23 11 53·2	A. D. T. (T)
47	δ Tau	3·9	D	1940 Jan. 20	21 37 15·7 **	H. E. B. (N); A. D. T. (T)
48	64 Tau	4·8	D	Jan. 20	22 28 28·0	A. D. T. (T)
799	B.D. −9° 5908	7·2	D	Oct. 11	19 44 23·3	A. D. T. (H)
800	B.D. −8° 5817	7·0	D	Oct. 11	23 17 19·3	H. E. B. (N)
810	B.D. −5° 5885	5·9	D	Oct. 12	22 27 11·4 **	H. E. B. (N); A. D. T. (H)
812	B.D. −5° 5894	6·4	D	Oct. 13	00 01 49·4	A. D. T. (H)
902 ††	B.D. +0° 19	6·9	D	1940 Nov. 10	23 10 47·5	A. D. T. (H)

** Mean of two observers.
†† Grazing occultation.

* *Observatory*, **64**, 31, 1941.
† By kind permission of the Director, University Observatory.

TABLE II

Serial No.	p	q	p^2	pq	q^2	$\Delta\sigma$	$p\Delta\sigma$	$q\Delta\sigma$
846	+77	+65	59	+49	41	−2·1	−1·6	−1·4
847	+81	+59	65	+48	35	−2·0	−1·6	−1·2
847	−90	+44	81	−40	19	+1·2	−1·1	+0·5
890	−97	+23	95	−22	5	−0·3	+0·3	−0·1
47	+94	−35	88	−33	12	−1·2	−1·1	+0·4
48	+59	−81	35	−48	65	+0·8	+0·5	−0·6
799	+70	+71	49	+50	51	−1·2	−0·9	−0·9
800	+68	+74	46	+50	54	−2·4	−1·6	−1·8
810	+91	−42	82	−38	18	−0·4	−0·4	+0·2
812	+73	−68	53	−50	47	−0·6	−0·4	+0·4
902 *	+27	−96	7	−26	93	−1·0	−0·3	+1·0

* Grazing occultation.